NASA TECHNICAL NOTE

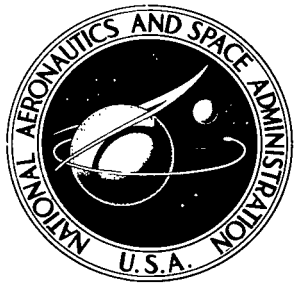

NASA TN D-6376

AN IMPROVED METHOD OF COLLOCATION FOR THE STRESS ANALYSIS OF CRACKED PLATES WITH VARIOUS SHAPED BOUNDARIES

by J. C. Newman, Jr.

Langley Research Center
Hampton, Va. 23365

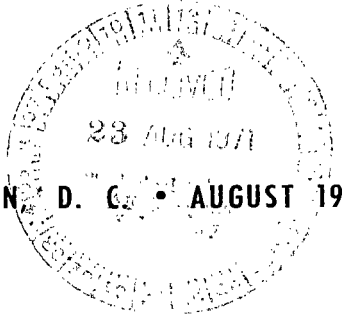

NATIONAL AERONAUTICS AND SPACE ADMINISTRATION • WASHINGTON, D. C. • AUGUST 1971

1. Report No.	2. Government Accession No.	3. Recipient's
NASA TN D-6376		

4. Title and Subtitle	5. Report Date
AN IMPROVED METHOD OF COLLOCATION FOR THE STRESS ANALYSIS OF CRACKED PLATES WITH VARIOUS SHAPED BOUNDARIES	August 1971
	6. Performing Organization Code
7. Author(s)	8. Performing Organization Report No.
J. C. Newman, Jr.	L-6996
	10. Work Unit No.
9. Performing Organization Name and Address	134-03-21-01
NASA Langley Research Center Hampton, Va. 23365	11. Contract or Grant No.
	13. Type of Report and Period Covered
12. Sponsoring Agency Name and Address	Technical Note
National Aeronautics and Space Administration Washington, D.C. 20546	14. Sponsoring Agency Code

15. Supplementary Notes

The information presented herein is based in part upon a thesis entitled "Stress Analysis of Simply and Multiply Connected Regions Containing Cracks by the Method of Boundary Collocation," offered in partial fulfillment of the requirements for the degree of Master of Science, Virginia Polytechnic Institute, Blacksburg, Virginia, May 1969.

16. Abstract

An improved method of boundary collocation was developed and applied to the two-dimensional stress analysis of cracks emanating from, or in the vicinity of, holes or boundaries of various shapes. The solutions, presented in terms of the stress-intensity factor, were based on the complex variable method of Muskhelishvili and a modified boundary-collocation method. The complex-series stress functions developed for simply and multiply connected regions containing cracks were constructed so that the boundary conditions on the crack surfaces are satisfied exactly. The conditions on the other boundaries were satisfied approximately by the modified collocation method. This improved method gave more rapid numerical convergence than other collocation techniques investigated.

17. Key Words (Suggested by Author(s))	18. Distribution Statement
Collocation Cracks Stress-intensity factors Stress analysis Numerical analysis	Unclassified – Unlimited

19. Security Classif. (of this report)	20. Security Classif. (of this page)	21. No. of Pages	22. Price*
Unclassified	Unclassified	45	$3.00

*For sale by the National Technical Information Service, Springfield, Virginia 22151

AN IMPROVED METHOD OF COLLOCATION FOR THE STRESS ANALYSIS OF CRACKED PLATES WITH VARIOUS SHAPED BOUNDARIES*

By J. C. Newman, Jr.
Langley Research Center

SUMMARY

An improved method of boundary collocation was developed and applied to the two-dimensional stress analysis of cracks emanating from, or in the vicinity of, holes or boundaries of various shapes. The solutions, presented in terms of the stress-intensity factor, were based on the complex variable method of Muskhelishvili and a modified boundary-collocation method. The complex-series stress functions developed for simply and multiply connected regions containing cracks were constructed so that the boundary conditions on the crack surfaces are satisfied exactly. The conditions on the other boundaries were satisfied approximately by the modified collocation method. This improved method gave more rapid numerical convergence than other collocation techniques investigated.

INTRODUCTION

In the life of a structure subjected to cyclic loads, cracks may initiate at and propagate from geometric discontinuities (holes, cut-outs, edges, or flaws). In designing structures for fatigue and fracture resistance the stresses around these sites must be calculated if unexpected failures are to be avoided. In recent years the use of high-strength (crack sensitive) materials for greater structural efficiency has resulted in a series of aircraft service failures due to the presence of small cracks. The rates at which these cracks propagate and the size of the crack that causes failure are strongly influenced by the shape of the discontinuity and the type of loads applied near it.

The crack-tip stress-intensity factor (restricted to small-scale yielding) can account for the influence of component configuration and loading on fatigue-crack growth

*The information presented herein is based in part upon a thesis entitled "Stress Analysis of Simply and Multiply Connected Regions Containing Cracks by the Method of Boundary Collocation," offered in partial fulfillment of the requirements for the degree of Master of Science, Virginia Polytechnic Institute, Blacksburg, Virginia, May 1969.

and static strength (refs. 1 to 4). Many investigators (refs. 5 to 12) have obtained theoretical stress-intensity factors for cracks growing near stress concentrations or boundaries. However, for cracks in complicated structures, stress-intensity factors cannot always be obtained by closed-form analytical methods. They are often obtained by a series solution (such as boundary collocation) which, to be useful, should converge rapidly to the proper answer.

The objective of this paper is to present an improved method of collocation for calculating the influence of various boundary shapes on the stress-intensity factor in two-dimensional linear elastic bodies and to apply this method to a number of boundary-value problems involving cracks.

Stress-intensity factors were calculated for cracks emanating from a circular hole in an infinite plate and cracks emanating from a circular hole in a finite plate, a crack near two circular holes in an infinite plate, a crack emanating from an elliptical hole in an infinite plate, and a crack in a finite plate. These configurations were subjected to either internally or externally applied loads.

SYMBOLS

A_n, B_n, C_n, D_n	coefficients in the complex stress functions
a	half crack length
b	half axis of the elliptical hole perpendicular to the plane of the crack
C_{jn}, D_{jn}	coefficients for jth pole in the complex stress functions
c	half axis of the elliptical hole, in the plane of the crack
d	distance from the centerline of the crack to the center of the circular hole
F	stress-intensity correction factor
F_x, F_y	resultant force per unit thickness acting in the x and y directions, respectively
F_{sn}, G_{sn}	sth influence function for nth coefficients
f,g	resultant forces and displacements

f_o, g_o	specified resultant forces or displacements on the boundary
H	height of rectangular plate
$i = \sqrt{-1}$	
K	stress-intensity factor
K_T	stress-concentration factor
M	number of points at which the error in the boundary conditions was evaluated
N	number of coefficients in each series stress function
P	concentrated force per unit thickness acting in the y direction
p	pressure
R	radius of the circular hole
r	minimum radius of curvature for the ellipse
S	stress on the external boundary
u,v	displacement in the x and y direction, respectively
W	width of rectangular plate
z	complex variable, $z = x + iy$
z_j	location of pole in x-y plane, $z_j = x_j + iy_j$
α	angle between the x-axis and the normal to a boundary
β	constant in equation (1)
ζ	coordinate along the contour of a boundary

κ	material constant
λ	ratio of applied stresses on separate portions of a boundary
μ	Lamé's constant (shear modulus)
ν	Poisson's ratio
σ_n	normal stress at a boundary
σ_x	normal stress in x direction
σ_y	normal stress in y direction
τ_{nt}	shear stress at a boundary
τ_{xy}	shear stress
Φ,Ψ,ϕ,Ω	complex stress functions

Subscripts:

j,m,n,q,s	indices

METHOD OF BOUNDARY COLLOCATION

Boundary collocation is a numerical method used to evaluate the unknown coefficients in a series stress function, such as those developed in appendix A. The method begins with a general series solution to the governing linear partial differential equation. Certain terms are eliminated from the series by conditions of symmetry. The series is then truncated to a specified number of terms. The coefficients are determined through satisfaction of prescribed boundary conditions. The series solution finally obtained satisfies the governing equation in the interior of the region exactly and one or more of the boundary conditions approximately.

Various techniques have been used to satisfy boundary conditions. Conway (ref. 13) determined the coefficients from the criterion that the boundary conditions be satisfied exactly at a specified number of points on the boundary. Hulbert (ref. 14) and Hooke (ref. 15) selected the coefficients so that the sum of the squares of the stress residuals was a minimum for a specified number of points on the boundary. These two techniques

have been used to analyze the stress state around a crack in a rectangular plate (refs. 11 and 14). Bowie (ref. 12) used a modified mapping-collocation technique to calculate the stress-intensity factors for a crack in a circular disk.

The present approach combines the complex variable method of Muskhelishvili (ref. 16) with a modified boundary-collocation method. The modification requires that the resultant forces on the boundary be specified (in a least-square sense) in contrast to previous work in which the boundary stresses were specified. (See appendix B.)

The resultant forces and displacements are expressed in terms of the complex stress functions $\phi(z)$ and $\Omega(z)$ (see appendix A) as

$$\beta\int \phi(z)dz + \int \Omega(\bar{z})dz + (z - \bar{z})\overline{\phi(z)} = f(x,y) + ig(x,y) \tag{1}$$

The bars denote the complex conjugates. For resultant forces ($\beta = 1$) acting over the arc $\zeta - \zeta_0$ on the boundary

$$F_y - iF_x = -\Big[f(x,y) + ig(x,y)\Big]\Big|_{\zeta_0}^{\zeta} \tag{2}$$

For convenience, the location of ζ_0 was selected as the intersection of the boundary with either the x- or y-axis. For displacements ($\beta = -\kappa$) at a point ζ on the boundary

$$2\mu(u + iv) = -\Big[f(x,y) + ig(x,y)\Big]_{z=\zeta} \tag{3}$$

For the case of plane strain $\kappa = 3 - 4\nu$ and for plane stress $\kappa = \dfrac{3 - \nu}{1 + \nu}$.

In general, the truncated complex stress functions can be expressed as

$$\left.\begin{aligned} \phi(z) &= \sum_{n=0}^{N} A_n \tilde{\phi}_n(z) \\ \Omega(z) &= \sum_{n=0}^{N} B_n \tilde{\Omega}_n(z) \end{aligned}\right\} \tag{4}$$

where $\tilde{\phi}_n$ and $\tilde{\Omega}_n$ are power-series functions of z. From equations (1) and (4) the expressions for f and g are

$$\left.\begin{aligned} f &= \sum_{n=0}^{N} A_n F_{1n} + \sum_{n=0}^{N} B_n F_{2n} \\ g &= \sum_{n=0}^{N} A_n G_{1n} + \sum_{n=0}^{N} B_n G_{2n} \end{aligned}\right\} \tag{5}$$

where F_{sn} and G_{sn} $(s = 1,2)$ are influence functions derived from $\tilde{\phi}_n$ and $\tilde{\Omega}_n$ for the nth coefficients.

Having developed the expressions for f and g in terms of the unknown coefficients A_n and B_n, it is necessary to select a method for evaluating the coefficients from the specified boundary conditions. The two methods developed for this purpose were (1) direct specification of boundary forces and/or displacements and (2) least-squares specification of boundary forces and/or displacements.

Direct Specification of Boundary Forces and/or Displacements

In specifying the resultant forces and/or displacements on the boundary, equations (5) were evaluated at N equally spaced points on the boundary and the resulting equations were solved on a computer for the unknown coefficients. Further details on the computer and matrix solutions are given in the section entitled "Application of the Boundary-Collocation Method."

Least-Squares Specification of Boundary Forces and/or Displacements

In general, the computed boundary values are in error at any given point ζ_m because the series stress functions were truncated. The square of this error is

$$e_m^2 = \left\{ f_o - \sum_{n=0}^{N} A_n F_{1n} - \sum_{n=0}^{N} B_n F_{2n} \right\}_m^2 + \left\{ g_o - \sum_{n=0}^{N} A_n G_{1n} - \sum_{n=0}^{N} B_n G_{2n} \right\}_m^2 \tag{6}$$

where f_o and g_o are specified boundary values at point ζ_m. The coefficients are then evaluated by minimizing the squares of the errors at a specified number of points M on the boundary:

$$\left.\begin{aligned} \frac{\partial \sum_{m=1}^{M} e_m^2}{\partial A_q} &= 0 \\ \frac{\partial \sum_{m=1}^{M} e_m^2}{\partial B_q} &= 0 \end{aligned}\right\} \tag{7}$$

where $q = 1,2,\ldots,N$. Equations (7) result in a set of $2N$ linear algebraic equations for the unknown coefficients A_n and B_n

$$\left.\begin{aligned} \sum_{n=0}^{N} \alpha_{nq} A_n + \sum_{n=0}^{N} \beta_{nq} B_n &= \delta_q \\ \sum_{n=0}^{N} \beta_{qn} A_n + \sum_{n=0}^{N} \gamma_{nq} B_n &= \eta_q \end{aligned}\right\} \tag{8}$$

where

$$\alpha_{nq} = \sum_{m=1}^{M} \left(F_{1n}F_{1q} + G_{1n}G_{1q}\right)_m$$

$$\beta_{nq} = \sum_{m=1}^{M} \left(F_{2n}F_{1q} + G_{2n}G_{1q}\right)_m$$

$$\gamma_{nq} = \sum_{m=1}^{M} \left(F_{2n}F_{2q} + G_{2n}G_{2q}\right)_m$$

$$\delta_q = \sum_{m=1}^{M} \left(f_o F_{1q} + g_o G_{1q}\right)_m$$

and

$$\eta_q = \sum_{m=1}^{M} \left(f_o F_{2q} + g_o G_{2q}\right)_m$$

The second partial derivative of the square of the error with respect to the unknown coefficients was positive, indicating a definite minimum.

APPLICATION OF THE BOUNDARY-COLLOCATION METHOD

The improved collocation method was used to analyze a number of crack problems. The configurations investigated were grouped into four categories: (1) cracks emanating from a circular hole in an infinite plate, (2) a crack near two circular holes in an infinite plate, (3) cracks emanating from an elliptical hole in an infinite plate, and (4) a crack in a finite plate. In each category several boundary conditions were investigated.

In applying the method, it was necessary to specify the points on the boundary at which the error equation was to be evaluated. The locations on the circular and elliptic boundaries were specified by dividing the angle θ_o into M equal increments ($\Delta\theta$) (see fig. 1). This procedure was selected because more points are concentrated on sections of the boundary which have smaller radii of curvature and, hence, larger stress gradients. For simplicity, this procedure was also employed on the external boundaries. In general, the value of M used in the solution of the various boundary-value problems was twice the total number of unknown coefficients in the series stress functions. For the case of cracks emanating from the elliptical hole in an infinite plate and from the circular hole in a finite plate, 160 coefficients were used in the stress functions. In all other cases 90 coefficients were used (except where noted).

A digital computer was used to solve the resulting equations using either single precision (14 significant digits) or double precision (29 significant digits). The equations

were solved by a routine which employed Jordan's method (ref. 17). Using single precision, the computer time was 1 and 4 minutes for solving 90 and 180 equations, respectively. Double precision required approximately twice as much time as single precision. Double precision was used only in the cases involving the finite plate.

The results are presented in terms of a correction factor F which accounts for the influence of the various boundaries on the stress-intensity factor for a crack in an infinite plate. The correction factor is defined as the ratio of the stress-intensity factor for the particular case to that for a crack in an infinite plate subjected to the same loading. A table of numerical values of F and the stress-intensity equation are given in Tables I to VII.

Cracks Emanating from a Circular Hole in an Infinite Plate

Remote biaxial stress.- For the case of cracks emanating from a circular hole, four collocation techniques were used to obtain the unknown coefficients in the stress functions. (See eqs. (A11) of appendix A.) The conditions at infinity were satisfied by adding to equations (A11) the $n = 0$ terms in equations (A10). The results of each of these techniques are compared in figure 2. The curves were obtained by specifying either stresses at discrete points on the boundary (stress equations) or resultant forces along the boundary (force equations), or by using a least-squares procedure with the stress equations or force equations. For the least-squares procedure employing resultant forces, two convergence curves are presented. One is for the case in which the number of points M was twice the total number of coefficients in the stress functions ($2N$ is the total number of coefficients in the stress functions); the other is for the case in which the number of points considered was five times the total number of coefficients. Convergence is seen to be rapid in both cases. For the least-squares procedure employing stress equations, the number of points considered was twice the total number of coefficients. All techniques seemed to converge to the same value as the number of coefficients increased. The value of F was approximately 2 percent higher than Bowie's approximate solution (ref. 5) for the same configuration and loading. The boundary stresses also converged to their specified values as the number of coefficients increased. However, the analysis using the least-squares procedure with the force equations converged more rapidly than the other techniques.

The correction factors for three states of biaxial stress are shown in figure 3. The solid curves show the results obtained in the present investigation. The circles are Bowie's solution and were obtained from a table given in reference 18. The agreement is considered good.

A solution for other values of λ was constructed by superposition of the two cases, $\lambda = 0$ and $\lambda = 1$. The stress-intensity equation is

$$K = S\sqrt{\pi a}\left[(1 - \lambda)F_0 + \lambda F_1\right] \tag{9}$$

where F_0 and F_1 are the correction factors for $\lambda = 0$ and $\lambda = 1$, respectively. The calculations for $\lambda = -1$ confirmed equation (9) to greater than eight significant digits. However, equation (9) is only valid for positive values of stress intensity. Negative stress intensities would indicate crack closure and the problem would become one of calculating contact stresses.

Internal pressure.- In a configuration like that in the preceding section, internal pressure p was applied to the hole boundary and λp to the crack surfaces. The stress functions for this case are given by equations (A11).

The correction factors for $\lambda = 0$ and $\lambda = 1$ are shown in figure 4. For the case in which no pressure is applied to the crack surfaces ($\lambda = 0$) the correction factor modifies the stress-intensity factor for wedge-force loading on the crack surfaces (ref. 18). Here the wedge-force loading $2pR$ is that produced by the internal pressure. The other case modifies the solution for a uniformly pressurized crack. A solution for other values was constructed by superposition of these two cases. The stress-intensity equation is

$$K = \frac{2pR}{\sqrt{\pi a}}(1 - \lambda)F_0 + \lambda p\sqrt{\pi a}\,F_1 \tag{10}$$

where F_0 and F_1 are the correction factors for $\lambda = 0$ and $\lambda = 1$, respectively. Equation (10) is also valid only for positive values of stress intensity. The results indicate that the influence of the hole on the stress-intensity equation may be neglected for values of a/R greater than 2.5.

A Crack Near Two Circular Holes in an Infinite Plate

Crack located between the holes subjected to remote uniaxial stress.- In the case of two circular holes the stress functions, equations (A13), were used with poles located at $z_j = \pm id$ (see appendix A). The conditions at infinity were satisfied by adding to equations (A13) the $n = 0$ terms in equations (A10).

The correction factors are shown in figure 5 for several values of d/R. At small d/R values the holes had a pronounced effect on the correction factors. However, for d/R values greater than 10 or a/R values greater than 3 the influence of the holes may be neglected.

In the limit as the crack length approaches zero, the correction factor is equivalent to the local-stress-concentration factor σ_y/S at the origin. In terms of the remote stress and the local stress the stress-intensity factors are

$$K = S\sqrt{\pi a}F = \sigma_y\sqrt{\pi a} \tag{11}$$

from which the correction factor is given as the ratio of σ_y to S. The circle plotted on the ordinate axis is the local-stress-concentration factor at the origin as given in reference 19 for a value of $\frac{d}{R} = 2$. The agreement is considered good.

Cracks approaching the holes subjected to remote uniaxial stress.- In this case the stress functions, equations (A13), were used with poles located at $z_j = \pm d$. Again, the conditions at infinity were satisfied by adding to equations (A13) the $n = 0$ terms in equations (A10).

The correction factors are shown in figure 6 for several values of d/R. The factors are plotted against the nondimensional crack length $\frac{a}{d - R}$. The correction factors increase from their initial value at $a = 0$ to large values as the crack approaches the edge of the hole. Again, the correction factor at $a = 0$ is equal to the local-stress-concentration factor at the point midway between the two holes.

As the crack intersects the boundary of the holes, the concept of the stress-intensity factor K no longer exists. However, the stress-concentration factor K_T at the edge of the hole ($x = R + d$) does describe the severity of the notch. The stress-concentration factors are shown in figure 7 as a function of R/d ratios. The stress-concentration factors were compared with those calculated from an "equivalent" elliptical-hole solution as shown by the dashed line. The elliptical hole had a minimum radius of curvature equal to the radius of the circular holes and had an overall length equal to $2(R + d)$. The stress-concentration factors for the elliptical hole were only slightly lower than those calculated for the case of two circular holes connected by a crack. Thus, the elliptical-hole solution may be used to approximate this configuration.

Cracks Emanating from an Elliptical Hole in an Infinite Plate

Remote uniaxial stress.- For the case of cracks emanating from an elliptical hole (see fig. 8) the stress functions, equations (A13), contained multiple poles z_j on either the x- or y-axis. The $n = 0$ terms in equations (A10) were added to equations (A13) in order to satisfy the boundary conditions at infinity. For the case of $\frac{b}{c} = 0.5$ and 2, the value of J in equations (A13) was 4 and for $\frac{b}{c} = 0.25$ and 4 the value was 16. These

values were determined by trial and error. The poles were always located on the major axis of the ellipse at the origin, at the center of the minimum curvature, and equally spaced between these points.

The correction factors are given in figure 8 for several values of b/c. The dashed curves show the theoretical limits expressed in terms of the correction factor F as the value of b approaches either zero or infinity. The stress-intensity factor in the limiting case ($b = \infty$) was obtained from reference 18 for the case of an edge crack in a semi-infinite plate. The other limit is where the elliptical hole reduces to a crack. The correction factors approached unity for all finite values of b/c as the crack length approached infinity. The edge-crack solution approached 1.12. For b/c ratios greater than 2 and large values of a/c the results indicated that the influence of the elliptical hole may not be negligible. However, for small b/c ratios the correction factor approached unity very rapidly.

Crack in a Finite Plate

In the following section the stress intensity solutions for two cases of a crack in a rectangular plate are presented. Double precision was used in the computer solution of the resulting equations primarily because the least-squares procedure generated matrix elements whose values ranged over many orders of magnitude and the unknown coefficients may have been susceptible to round-off error. In fact, for some choices of the pertinent parameters the single-precision routine did not appear to converge. However, for the same parameters the double-precision routine did appear to converge as the number of coefficients increased.

Crack subjected to wedge-force loading.- For the case of a crack in a rectangular plate subjected to wedge-force loading on the crack surfaces (see fig. 9) the stress functions were taken to be

$$\left.\begin{aligned} \phi(z) &= \phi_0(z) + \frac{Pa}{2\pi z\sqrt{z^2 - a^2}} \\ \Omega(z) &= \Omega_0(z) + \frac{Pa}{2\pi z\sqrt{z^2 - a^2}} \end{aligned}\right\} \tag{12}$$

where ϕ_0 and Ω_0 are given by equations (A10). The additional terms in equations (12) were added in order to account for the concentrated forces on the crack surfaces (ref. 9). The unknown coefficients from equations (A10) in equations (12) were evaluated by

satisfying the conditions on the external boundary. To show convergence, an example problem with $\frac{2a}{W} = 0.9$ was solved for several values of 2N (see fig. 9). This example problem was selected because the close proximity of the crack tip to the boundary was expected to pose difficulties in achieving convergence. However, the convergence was rapid.

The correction factors for several values of H/W are shown in figure 10. For a given value of H/W the correction factors ranged from unity, at small crack length to plate width ratios, to very large values at large ratios.

In figure 11, a comparison is made between experimental and theoretical stress-intensity correction factors for a wedge-force loaded panel. The material was 7075-T6 aluminum alloy cycled at constant amplitude with a load ratio (minimum load to maximum load) of 0.05. The experimental stress-intensity factors were obtained from measured crack growth rates used together with a curve of stress intensity as a function of crack growth rate (ref. 4). The agreement between the calculated and the experimental correction factors is considered good.

Cracks emanating from a circular hole subjected to uniaxial stress.- For the case of cracks growing from a circular hole in a rectangular plate subjected to a uniaxial stress (see fig. 12) the stress functions were taken to be the sum of equations (A10) and (A11) since both internal and external boundaries must be considered. The unknown coefficients were evaluated by satisfying the conditions on both boundaries.

The correction factors for several values of 2R/W and a plate aspect ratio (H/W) of 2 are shown in figure 12. As the hole radius approaches zero, the boundary-value problem reduces to that of a single crack in a rectangular plate. In this case all coefficients in equation (A11) are set equal to zero. The correction factors shown for $\frac{2R}{W} = 0$ agree almost identically with Isida's solution (ref. 20) for the case of a central crack in a finite width strip. The solid curve was slightly higher than Isida's solution for values of $\frac{2a}{W} > 0.7$. However, the difference may be due to the influence of the finite height.

CONCLUDING REMARKS

An improved method of boundary collocation was presented and applied to the stress analysis of cracked plates having various boundary shapes and subjected to inplane loading. The solutions were based on the complex variable method of Muskhelishvili and a modification of the numerical method of boundary collocation. The complex series stress functions formulated for cracked plates automatically satisfy the boundary conditions on the crack surfaces. The conditions on the other boundaries were satisfied approximately by the series solution. Stress-intensity correction factors were presented

for several configurations involving cracks in the presence of stress concentrations or boundaries. The least-squares boundary-collocation method used to minimize the resultant-force residuals on the boundary gave better numerical convergence in the boundary conditions than the other three collocation methods investigated. The other methods were (1) direct specification of boundary forces, (2) direct specification of boundary stresses at discrete points, and (3) least-squares specification of boundary stresses. The improved method was able to analyze more complex boundary-value problems than the other methods because of the more rapid convergence in the series solution.

The stress-intensity factors presented in this paper cover a moderate range of configurations and loadings. Most of the boundary-value problems solved do occur frequently in aircraft structures such as cracks growing from or near cutouts (windows, rivet holes, etc.) or from other structural discontinuities. Thus, the solutions presented here may be used to design a structure more efficient against fatigue and fracture or to help monitor structural damage due to fatigue loading.

Langley Research Center,
National Aeronautics and Space Administration,
Hampton, Va., June 15, 1971.

APPENDIX A

FORMULATION OF THE COMPLEX SERIES STRESS FUNCTIONS FOR CRACKED BODIES

One of the major advances in the field of two-dimensional linear elasticity has been the complex-variable approach of Muskhelishvili (ref. 16). The representation of biharmonic functions by analytic functions has led to a general method of solving plane-strain and generalized plane-stress problems.

The following formulation for two-dimensional cracked bodies is based on the work of Muskhelishvili for an infinite plane region containing cracks and subjected to inplane loading (see fig. 13). The known surface tractions are applied to the boundaries of this region. The body forces are assumed to be zero and the material is assumed to be linear elastic, isotropic, and homogeneous. The equilibrium and compatibility equations are combined to form the biharmonic equation

$$\frac{\partial^4 U}{\partial x^4} + 2\frac{\partial^4 U}{\partial x^2\,\partial y^2} + \frac{\partial^4 U}{\partial y^4} = 0 \tag{A1}$$

where $U(x,y)$ is the Airy stress function.

The biharmonic function $U(x,y)$ can be expressed as

$$U(x,y) = \frac{1}{2}\,\mathrm{Re}\left[\int \overline{\Psi}(z)\,dz + \int \Phi(z)dz + (\bar{z} - z)\Phi(z)\right] \tag{A2}$$

where $\Phi'(z) = \phi(z)$ and $\Psi'(z) = \Omega(z)$. The primes and bars denote differentiation and complex conjugates, respectively. Therefore, the generalized plane-stress and plane-strain problems are reduced to the determination of these functions subject to specified boundary conditions.

From reference 16, the stress functions in the neighborhood of a crack $(z = \pm a)$ can be expressed as

$$\left.\begin{aligned} \phi(z) &= \frac{Q_1(z)}{\sqrt{z^2 - a^2}} + Q_2(z) \\ \Omega(z) &= \frac{Q_3(z)}{\sqrt{z^2 - a^2}} + Q_4(z) \end{aligned}\right\} \tag{A3}$$

where

$$Q_s(z) = \sum_{n=-\infty}^{\infty} A_{sn} z^n \tag{A4}$$

In the present investigation, the formulation of the complex series stress functions for simply and multiply connected regions containing cracks was restricted to the situation where the configuration and loading are symmetric about the x- and y-axis. The boundary conditions satisfied by ϕ and Ω for a stress-free crack surface are

$$\left.\begin{array}{ll} \text{(I)} \quad \sigma_y = \tau_{xy} = 0 & \left(|x| < a; \quad y = 0\right) \\ \text{(II)} \quad \tau_{xy} = v = 0 & \left(|x| \geq a; \quad y = 0\right) \\ \text{(III)} \quad \tau_{xy} = u = 0 & \left(|y| \geq 0; \quad x = 0\right) \end{array}\right\} \tag{A5}$$

where the coordinate system used is shown in figure 13. The stresses expressed in terms of the stress functions are

$$\left.\begin{array}{l} \sigma_x + \sigma_y = 2\left[\phi(z) + \overline{\phi(z)}\right] \\ \sigma_y - \sigma_x + 2i\tau_{xy} = 2\left[(\bar{z} - z)\phi'(z) - \phi(z) + \overline{\Omega}(z)\right] \end{array}\right\} \tag{A6}$$

The displacements are given by equation (1).

The boundary conditions in equations (A5) define a unique relationship between the two analytic functions ϕ and Ω. The relationship for the series which contains the square-root term is $Q_1(z) = Q_3(z)$ and for the series which contains no square-root term, $Q_2(z) = -Q_4(z)$. These conditions insure the satisfaction of the boundary conditions (stress free) on the crack surfaces.

For a multiply connected region, in addition to the boundary conditions stated in equations (A5), the single-valuedness of displacements must be insured. This condition is stated as

$$\kappa \oint_{\Lambda_j} \phi(z)dz - \oint_{\Lambda_j} \Omega(\bar{z})d\bar{z} = 0 \tag{A7}$$

where Λ_j is the contour around each separate hole boundary L_j (see fig. 13).

The stress intensity factor K is obtained from the stress functions as

$$K = 2\sqrt{2\pi} \lim_{z \to a} \sqrt{z - a}\ \phi(z) \tag{A8}$$

As an example, consider a crack located along the x-axis in an infinite plate as shown in figure 14. The dashed lines L_0 and L_1 define the boundaries of the region (shaded area). The internal boundary L_1 has cracks growing from the edge of the hole to $x = \pm a$. The boundaries L_0 and L_1 may have any simple shape which is symmetric about the x- and y-axis and be subjected to any symmetric boundary conditions. The complex-series stress functions must be single-valued and analytic in the region between L_0 and L_1. This region does not include the crack which is represented by a branch cut. The stress functions are

$$\left.\begin{aligned} \phi(z) &= \phi_0(z) + \phi_1(z) \\ \Omega(z) &= \Omega_0(z) + \Omega_1(z) \end{aligned}\right\} \tag{A9}$$

The subscripts denote the functions which are used to satisfy the boundary conditions on boundaries L_0 and L_1, respectively. The stress functions used to satisfy the conditions on the external boundary L_0 are

$$\left.\begin{matrix} \phi_0(z) \\ \Omega_0(z) \end{matrix}\right\} = \frac{z}{\sqrt{z^2 - a^2}} \sum_{n=0}^{N} A_n z^{2n} \pm \sum_{n=0}^{N} B_n z^{2n} \tag{A10}$$

where the coefficients A_n and B_n are real. In the situation where the boundary L_0 is located at infinity $A_0 = \frac{S}{2}$, $B_0 = \frac{S}{4}(\lambda - 1)$ and the remaining coefficients for $n \geq 1$ are zero. For the internal boundary L_1 the stress functions are

$$\left.\begin{matrix} \phi_1(z) \\ \Omega_1(z) \end{matrix}\right\} = \frac{z}{\sqrt{z^2 - a^2}} \sum_{n=1}^{N} \frac{C_n}{z^{2n}} \pm \sum_{n=1}^{N} \frac{D_n}{z^{2n}} \tag{A11}$$

where the coefficients C_n and D_n are real. The stress functions, equations (A10) and (A11), automatically satisfy the boundary conditions on the crack surfaces. The conditions on the other boundaries $(L_0$ and $L_1)$ were approximated by the series solution. The stress-intensity factor K calculated from equations (A8), (A10), and (A11) is

$$K = \sqrt{\pi a} \left\{ \sum_{n=0}^{N} 2A_n a^{2n} + \sum_{n=1}^{N} \frac{2C_n}{a^{2n}} \right\} \tag{A12}$$

In the case of multiple circular holes or elliptical holes, the complex-series stress functions require the use of poles at various stations along the x- or y-axis. The stress functions are given by

$$\left.\begin{matrix}\phi(z)\\ \Omega(z)\end{matrix}\right\} = \frac{z}{\sqrt{z^2 - a^2}} \sum_{j=1}^{J} \sum_{n=1}^{N} \frac{C_{jn}}{\left(z^2 - z_j^2\right)^n} \pm \sum_{j=1}^{J} \sum_{n=1}^{N} \frac{D_{jn}}{\left(z^2 - z_j^2\right)^n} \tag{A13}$$

where the coefficients C_{jn} and D_{jn} are real. In these stress functions the poles $\pm z_j$ must lie on either the x- or y-axis and be symmetrically placed about the other axis.

APPENDIX B

OTHER COLLOCATION METHODS INVESTIGATED

Direct Specification of Boundary Stresses

The boundary-collocation method treated in this section involves the specification of the normal- and shear-stress components at discrete points on the boundary. The boundary-value problem considered had cracks emanating from the edges of a circular hole in an infinite plate subjected to a biaxial stress (see fig. 15). The complex equation for the two stress components on the boundary is

$$\sigma_n - i\tau_{nt} = \phi(z) + \overline{\phi(z)} - \left[(\bar{z} - z)\phi'(z) - \phi(z) + \overline{\Omega}(z)\right]e^{2i\alpha} \tag{B1}$$

where the stress functions are

$$\left.\begin{matrix}\phi(z)\\ \Omega(z)\end{matrix}\right\} = \frac{z}{\sqrt{z^2 - a^2}} \sum_{n=0}^{N} \frac{C_n}{z^{2n}} \pm \sum_{n=0}^{N} \frac{D_n}{z^{2n}} \tag{B2}$$

The coefficients C_0 and D_0 were determined from the stress conditions at infinity. The remaining coefficients were determined from the conditions that $\sigma_n = 0$ and $\tau_{nt} = 0$ at N equally spaced points on the boundary. The resulting equations were solved on a computer using single precision. The stress-intensity factor was calculated from equation (A8) as

$$K = S\sqrt{\pi a}\left[1 + \sum_{n=1}^{N} \frac{2C_n}{a^{2n}}\right] \tag{B3}$$

where the term in the brackets is the correction factor F.

Least-Squares Specification of Boundary Stresses

The boundary-collocation method described in this section is similar to the one in the preceding section, except that here more equations are written in terms of the stress boundary conditions than there are unknown coefficients. The coefficients are then chosen so as to minimize the sum of the stress residuals on the boundary at a specified number of points M. The normal stress and shear stress components expressed in terms of the stress functions (eqs. (B2)) are

$$\left.\begin{aligned}\sigma_n &= \sum_{n=0}^{N} C_n F_{1n} + \sum_{n=0}^{N} D_n F_{2n} \\ \tau_{nt} &= \sum_{n=0}^{N} C_n G_{1n} + \sum_{n=0}^{N} D_n G_{2n}\end{aligned}\right\} \tag{B4}$$

where F_{sn} and G_{sn} $(s = 1,2)$ are the influence functions derived from the stress functions for the respective coefficient. Again, the coefficients C_0 and D_0 are determined from the stress conditions at infinity. Since the circular boundary is stress free, the square of the error in the boundary condition at point ζ_m is

$$e_m{}^2 = \left\{\sum_{n=0}^{N} C_n F_{1n} + \sum_{n=0}^{N} D_n F_{2n}\right\}_m^2 + \left\{\sum_{n=0}^{N} C_n G_{1n} + \sum_{n=0}^{N} D_n G_{2n}\right\}_m^2 \tag{B5}$$

The coefficients were then selected so that the sum of the squares of the errors at a number of points M on the boundary was a minimum

$$\left.\begin{aligned}\frac{\partial \sum_{m=1}^{M} e_m{}^2}{\partial C_q} &= 0 \\ \frac{\partial \sum_{m=1}^{M} e_m{}^2}{\partial D_q} &= 0\end{aligned}\right\} \tag{B6}$$

where $q = 1,2,\ldots,N$. Equation (B6) results in a set of $2N$ linear algebraic equations for C_n and D_n

$$\left.\begin{aligned} \sum_{n=0}^{N} \alpha_{nq} C_n + \sum_{n=0}^{N} \beta_{nq} D_n = 0 \\ \sum_{n=0}^{N} \beta_{qn} C_n + \sum_{n=0}^{N} \gamma_{nq} D_n = 0 \end{aligned}\right\} \tag{B7}$$

where

$$\alpha_{nq} = \sum_{m=1}^{M} \left(F_{1n}F_{1q} + G_{1n}G_{1q}\right)_m$$

$$\beta_{nq} = \sum_{m=1}^{M} \left(F_{2n}F_{1q} + G_{2n}G_{1q}\right)_m$$

and

$$\gamma_{nq} = \sum_{m=1}^{M} \left(F_{2n}F_{2q} + G_{2n}G_{2q}\right)_m$$

These equations were solved on a computer using single precision. The resulting coefficients were used in equation (B3) to calculate the stress-intensity factor.

REFERENCES

1. Paris, Paul C.; Gomez, Mario D.; and Anderson, William E.: A Rational Analytic Theory of Fatigue. Trend Eng. (Univ. of Washington), vol. 13, no. 1, Jan. 1961, pp. 9-14.

2. Donaldson, D. R.; and Anderson, W. E.: Crack Propagation Behavior of Some Airframe Materials. D6-7888, Paper presented at Crack Propagation Symposium (Cranfield, England), Sept. 1961.

3. Anon.: Fracture Testing of High-Strength Sheet Materials: A Report of a Special ASTM Committee. ASTM Bull., no. 243, Jan 1960, pp. 29-40.

4. Figge, I. E.; and Newman, J. C., Jr.: Prediction of Fatigue-Crack-Propagation Behavior in Panels With Simulated Rivet Forces. NASA TN D-4702, 1968.

5. Bowie, O. L.: Analysis of an Infinite Plate Containing Radial Cracks Originating at the Boundary of an Internal Circular Hole. J. Math. Phys., vol. XXXV, no. 1, Apr. 1956, pp. 60-71.

6. Grebenkin, G. G.; and Kaminskii, A. A.: Propagation of Cracks Near an Arbitrary Curvilinear Hole. Sov. Mater. Sci., vol. 3, no. 4, July-Aug. 1967, pp. 340-344.

7. Fichter, W. B.: Stresses at the Tip of a Longitudinal Crack in a Plate Strip. NASA TR R-265, 1967.

8. Isida, M.: On the Determination of Stress Intensity Factors for Some Common Structural Problems. Eng. Fracture Mech., vol. 2, no. 1, July 1970, pp. 61-79.

9. Erdogan, Fazil: On the Stress Distribution in Plates With Collinear Cuts Under Arbitrary Loads. Proceedings of the Fourth U.S. National Congress of Applied Mechanics, Vol. One, Amer. Soc. Mech. Eng., 1962, pp. 547-553.

10. Hulbert, L. E.; Hahn, G. T.; Rosenfield, A. R.; and Kanninen, M. F.: An Elastic-Plastic Analysis of a Crack in a Plate of Finite Size. Applied Mechanics, M. Hetényi and W. G. Vincenti, eds., Springer-Verlag, 1969, pp. 221-235.

11. Kobayashi, A. S.; Cherepy, R. D.; and Kinsel, W. C.: A Numerical Procedure for Estimating the Stress Intensity Factor of a Crack in a Finite Plate. Trans. ASME, Ser. D.: J. Basic Eng., vol. 86, no. 4, Dec. 1964, pp. 681-684.

12. Bowie, O. L.; and Neal, D. M.: A Modified Mapping-Collocation Technique for Accurate Calculation of Stress Intensity Factors. Int. J. Fracture Mech., vol. 6, no. 2, June 1970, pp. 199-206.

13. Conway, H. D.: The Approximate Analysis of Certain Boundary-Value Problems. Trans. ASME, Ser. E: J. Appl. Mech., vol. 27, no. 2, June 1960, pp. 275-277.

14. Hulbert, Lewis Eugene: The Numerical Solution of Two-Dimensional Problems of the Theory of Elasticity. Bull. 198, Eng. Exp. Sta., Ohio State Univ.

15. Hooke, C. J.: Numerical Solution of Plane Elastostatic Problems By Point Matching. J. Strain Anal., vol. 3, no. 2, Apr. 1968, pp. 109-114.

16. Muskhelishvili, N. I. (J. R. M. Radok, transl.): Some Basic Problems of the Mathematical Theory of Elasticity. Third ed., P. Noordhoff, Ltd. (Groningen), 1953.

17. Fox, L.: An Introduction to Numerical Linear Algebra. Oxford Univ. Press, 1965.

18. Paris, Paul C.; and Sih, George C.: Stress Analysis of Cracks. Fracture Toughness Testing and Its Applications, Spec. Tech. Publ. No. 381, Amer. Soc. Testing Mater., c.1965, pp. 30-83.

19. Savin, G. N. (Eugene Gros, transl.): Stress Concentration Around Holes. Pergamon Press, Inc., 1961.

20. Isida, M.: On the Tension of a Strip With a Central Elliptical Hole. Trans. Japan Soc. Mech. Engrs., vol. 21, no. 107, 1955, p. 511.

TABLE I.- CRACKS EMANATING FROM A CIRCULAR HOLE IN AN INFINITE PLATE SUBJECTED TO BIAXIAL STRESS

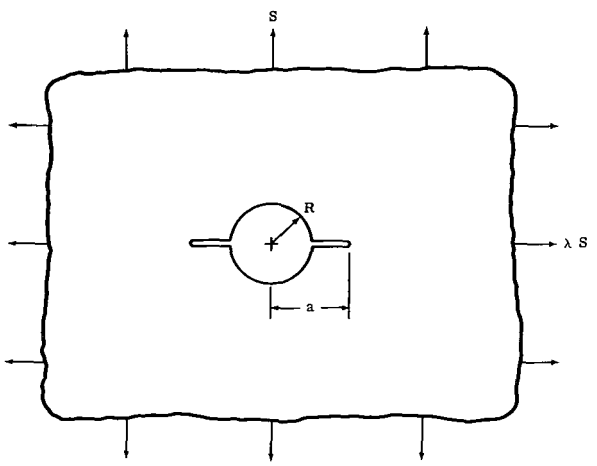

$K = S\sqrt{\pi a}\ F$

$2N = 120$

a/R	F (λ=-1)	F_0 (λ=1)	F_1 (λ=0)
1.01	0.4325	0.3256	0.2188
1.02	.5971	.4514	.3058
1.04	.7981	.6082	.4183
1.06	.9250	.7104	.4958
1.08	1.0135	.7843	.5551
1.10	1.0775	.8400	.6025
1.15	1.1746	.9322	.6898
1.20	1.2208	.9851	.7494
1.25	1.2405	1.0168	.7929
1.30	1.2457	1.0358	.8259
1.40	1.2350	1.0536	.8723
1.50	1.2134	1.0582	.9029
1.60	1.1899	1.0571	.9242
1.80	1.1476	1.0495	.9513
2.00	1.1149	1.0409	.9670
2.20	1.0904	1.0336	.9768
2.50	1.0649	1.0252	.9855
3.00	1.0395	1.0161	.9927
4.00	1.0178	1.0077	.9976

TABLE II.- CRACKS EMANATING FROM AN INTERNALLY PRESSURIZED HOLE IN AN INFINITE PLATE

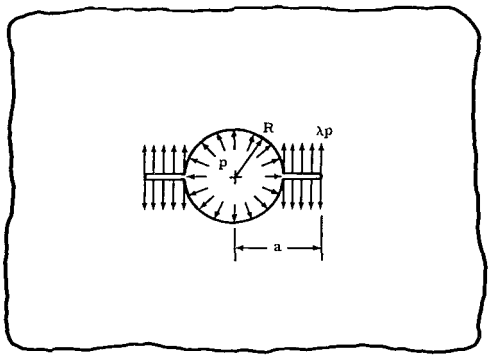

For $\lambda = 1$, $K = p\sqrt{\pi a}\, F_1$

For $\lambda = 0$, $K = \frac{2pR}{\sqrt{\pi a}}\, F_0$

$2N = 120$

a/R	F_1 (λ=1)	F_0 (λ=0)
1.01	0.2188	0.1725
1.02	.3058	.2319
1.04	.4183	.3334
1.06	.4958	.3979
1.08	.5551	.4485
1.10	.6025	.4897
1.15	.6898	.5688
1.20	.7494	.6262
1.25	.7929	.6701
1.30	.8259	.7053
1.40	.8723	.7585
1.50	.9029	.7971
1.60	.9242	.8264
1.80	.9513	.8677
2.00	.9670	.8957
2.20	.9768	.9154
2.50	.9855	.9358
3.00	.9927	.9566
4.00	.9976	.9764

TABLE III.- CRACK LOCATED BETWEEN TWO CIRCULAR HOLES
IN AN INFINITE PLATE SUBJECTED TO UNIAXIAL STRESS

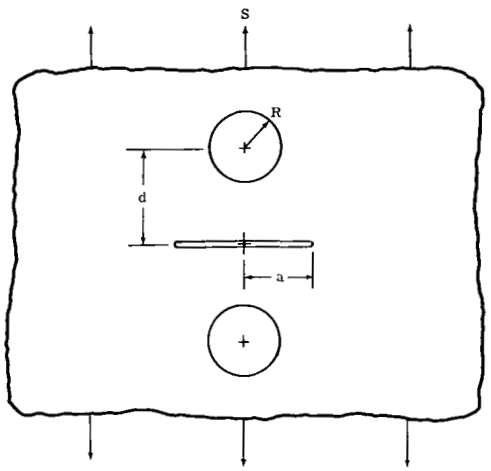

$$K = S\sqrt{\pi a}\ F$$

a/R	$F\left(\frac{d}{R}=2\right)$	$F\left(\frac{d}{R}=3\right)$	$F\left(\frac{d}{R}=4\right)$	$F\left(\frac{d}{R}=6\right)$	$F\left(\frac{d}{R}=10\right)$
0.01	0.1390	0.5234	0.7127	0.8661	0.9506
.25	.1728	.5355	.7172	.8671	------
.50	.2683	.5698	.7303	.8700	.9512
.75	.4045	.6206	.7505	.8748	------
1.00	.5502	.6799	.7758	.8810	.9528
1.50	.7809	.7958	.8324	.8969	.9553
2.00	.9058	.8819	.8847	.9150	.9585
2.50	.9640	.9351	.9250	.9328	.9622
3.00	.9902	.9654	.9527	.9486	.9663

TABLE IV.- CRACK APPROACHING TWO CIRCULAR HOLES IN AN INFINITE PLATE SUBJECTED TO UNIAXIAL STRESS

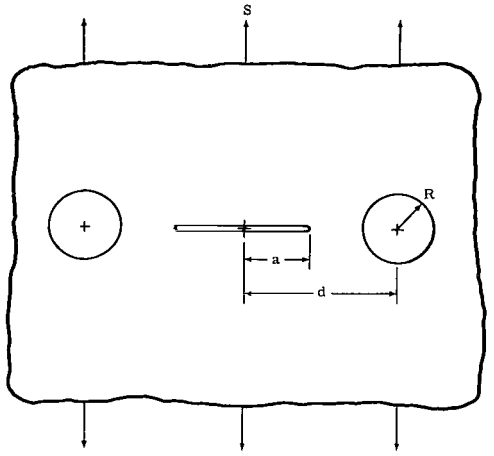

$K = S\sqrt{\pi a}\ F$

$\frac{a}{d - R}$	$F\left(\frac{d}{R}=1.15\right)$	$F\left(\frac{d}{R}=1.25\right)$	$F\left(\frac{d}{R}=1.5\right)$	$F\left(\frac{d}{R}=2\right)$	$F\left(\frac{d}{R}=4\right)$
0.01	4.3975	3.2630	2.1530	1.4687	1.0761
.1	4.4160	3.2739	2.1612	1.4738	1.0774
.2	4.4751	3.3143	2.1875	1.4898	1.0816
.3	4.5853	3.3856	2.2338	1.5183	1.0892
.4	4.7308	3.4946	2.3045	1.5624	1.1017
.5	4.9593	3.6538	2.4076	1.6279	1.1215
.6	5.2890	3.8850	2.5575	1.7249	1.1538
.7	5.7816	4.2271	2.7824	1.8740	1.2101
.8	-----	4.7825	3.1504	2.1230	1.3202
.9	-----	5.8028	3.8661	2.6350	1.5927

TABLE V.- CRACKS EMANATING FROM AN ELLIPTICAL HOLE
IN AN INFINITE PLATE SUBJECTED TO UNIAXIAL STRESS

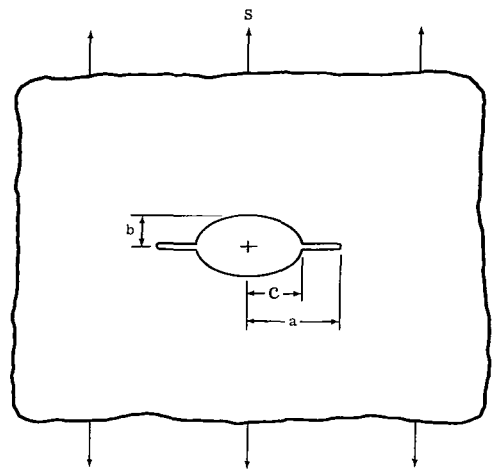

$K = S\sqrt{\pi a}\ F$

a/c	$F\left(\frac{b}{c}=0.25\right)$	$F\left(\frac{b}{c}=0.5\right)$	$F\left(\frac{b}{c}=1\right)$	$F\left(\frac{b}{c}=2\right)$	$F\left(\frac{b}{c}=4\right)$
1.02	0.9050	0.6757	0.4514	0.3068	0.2114
1.03	.9597	.7742	-----	-----	-----
1.04	.9865	.8398	.6082	.4297	-----
1.05	1.0013	.8861	-----	-----	.3137
1.06	1.0098	.9206	.7104	.5164	-----
1.08	1.0179	.9664	.7843	.5843	.4463
1.10	1.0206	.9925	.8400	.6401	.5027
1.15	1.0202	1.0258	.9322	.7475	.5901
1.20	1.0176	1.0357	.9851	.8241	-----
1.25	-----	-----	-----	-----	.7248
1.30	-----	1.0366	1.0358	.9255	-----
1.40	-----	1.0317	1.0536	.9866	.8494
1.50	-----	-----	1.0582	1.0246	-----
1.55	-----	-----	-----	-----	.9279
1.60	-----	-----	1.0571	1.0483	-----
1.80	-----	-----	1.0495	1.0714	1.0063
2.00	-----	-----	1.0409	1.0777	-----
2.10	-----	-----	-----	-----	1.0551
2.20	-----	-----	1.0336	1.0766	-----
2.40	-----	-----	1.0251	1.0722	1.0788

TABLE VI.- WEDGE-FORCE LOADED CRACK
IN A RECTANGULAR PLATE

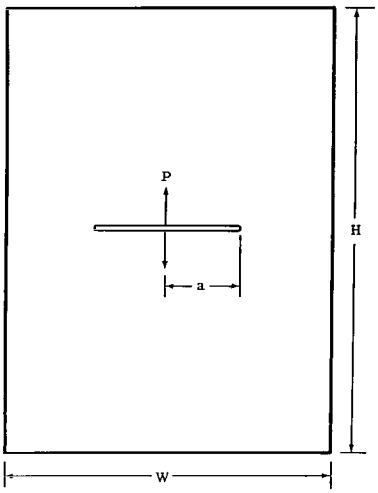

$$K = \frac{P}{\sqrt{\pi a}} F$$

2a/W	$F\left(\frac{H}{W}=0.5\right)$	$F\left(\frac{H}{W}=0.75\right)$	$F\left(\frac{H}{W}=1.0\right)$	$F\left(\frac{H}{W}=2.0\right)$
0	1.0000	1.0000	1.0000	1.0000
.1	1.0921	1.0467	1.0279	1.0121
.2	1.3572	1.1863	1.1115	1.0497
.3	1.7721	1.4185	1.2499	1.1163
.4	2.3269	1.7431	1.4418	1.2191
.5	3.0554	2.1589	1.6866	1.3710
.6	4.0464	2.6587	1.9894	1.5958
.7	5.3985	3.2275	2.3772	1.9421
.8	7.0162	3.8858	2.9523	2.5309
.9	8.4078	4.9791	4.1665	3.7810

TABLE VII.- CRACKS EMANATING FROM A CIRCULAR HOLE IN A RECTANGULAR PLATE SUBJECTED TO UNIAXIAL STRESS

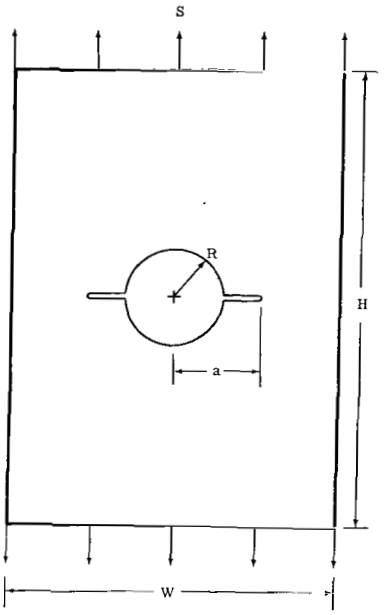

$K = S\sqrt{\pi a}\ F$

$\frac{H}{W} = 2$

2a/W	F $\left(\frac{2R}{W}=0\right)$
0	1.0000
.1	1.0061
.2	1.0249
.3	1.0583
.4	1.1102
.5	1.1876
.6	1.3043
.7	1.4891
.8	1.8161
.9	2.5482

2a/W	F $\left(\frac{2R}{W}=0.25\right)$
0.25	0
.26	.6593
.27	.8510
.28	.9605
.29	1.0304
.30	1.0776
.35	1.1783
.40	1.2156
.50	1.2853
.60	1.3965
.70	1.5797
.80	1.9044
.85	2.1806
.90	2.6248

2a/W	F $\left(\frac{2R}{W}=0.5\right)$
0.50	0
.51	.6527
.52	.8817
.525	.9630
.53	1.0315
.54	1.1426
.55	1.2301
.60	1.5026
.70	1.8247
.78	2.1070
.85	2.4775
.90	2.9077

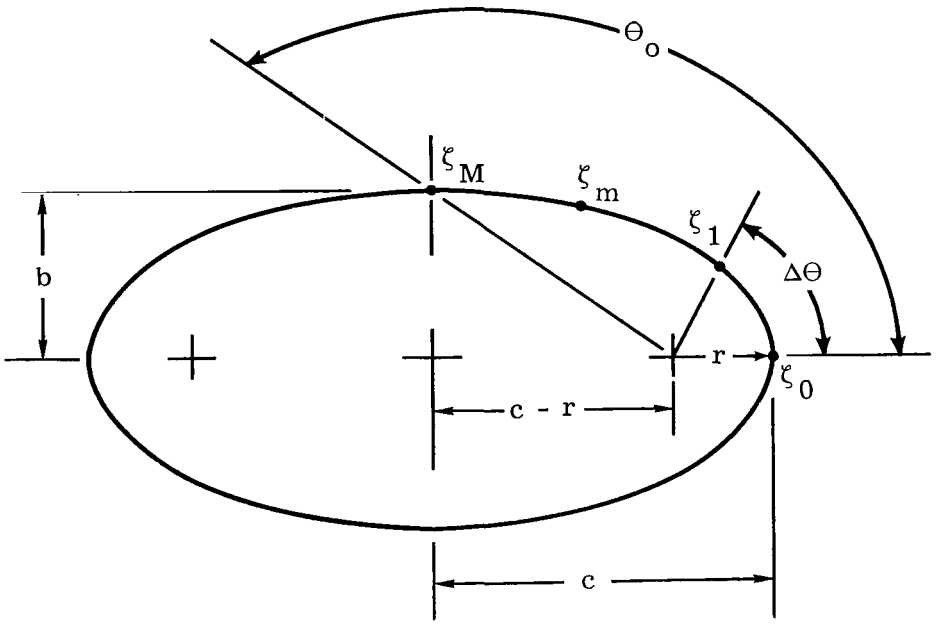

Figure 1.- Coordinate system used for describing the location of the collocation points on the circular and elliptic boundaries.

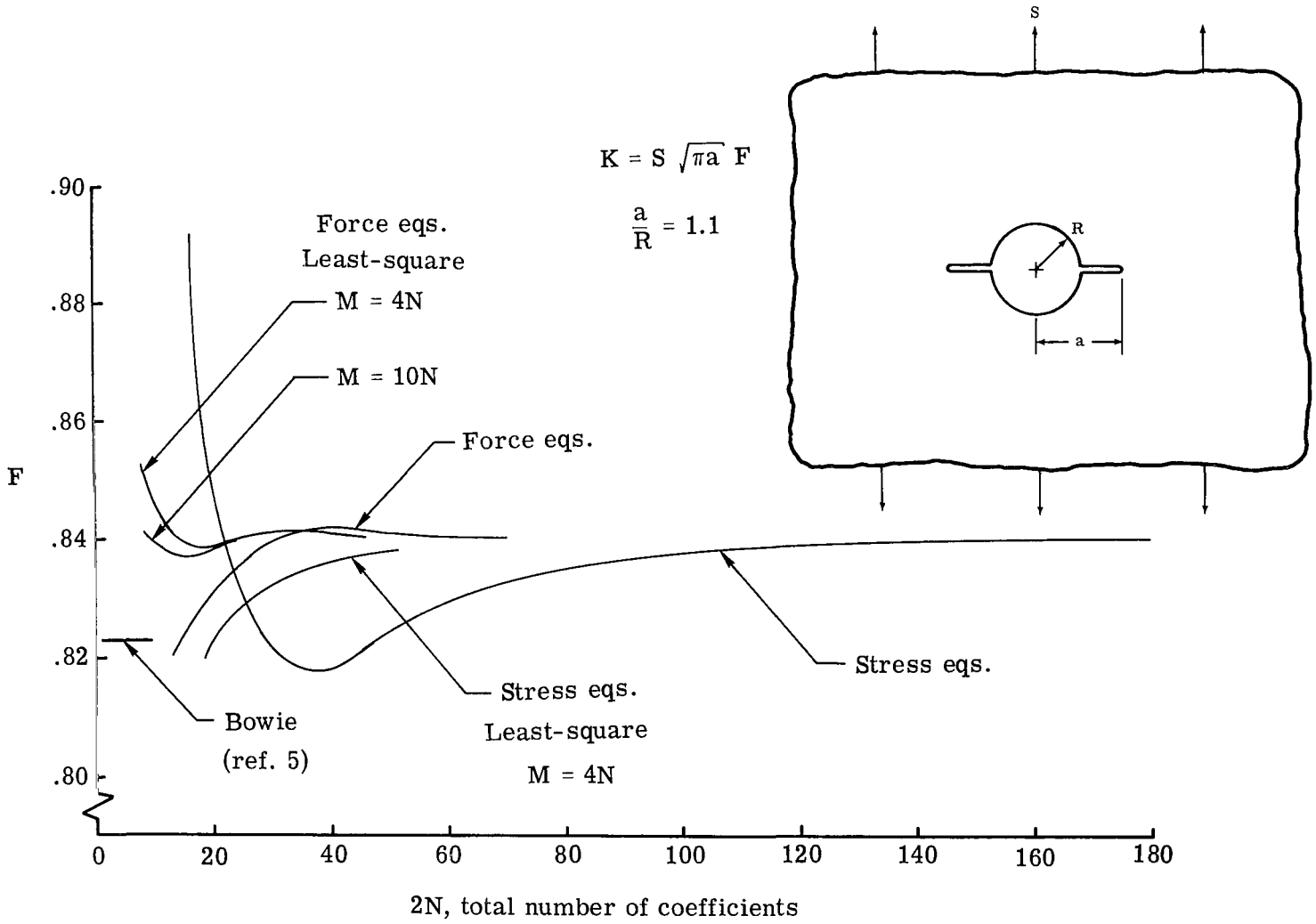

Figure 2.- Convergence curves for the problem of cracks emanating from a circular hole in an infinite plate subjected to uniaxial stress.

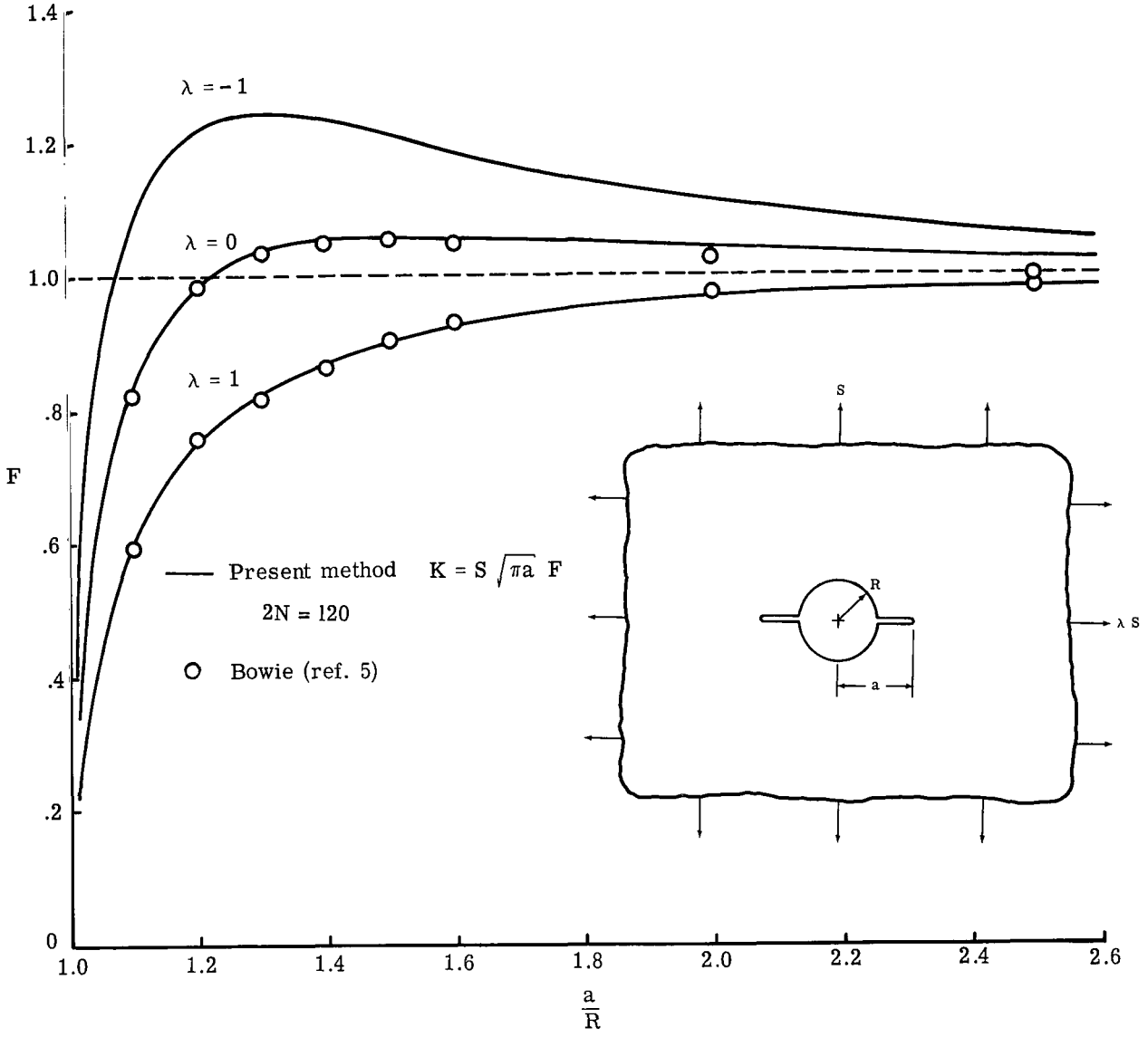

Figure 3.- Stress-intensity correction factors for cracks emanating from a circular hole in an infinite plate subjected to biaxial stress.

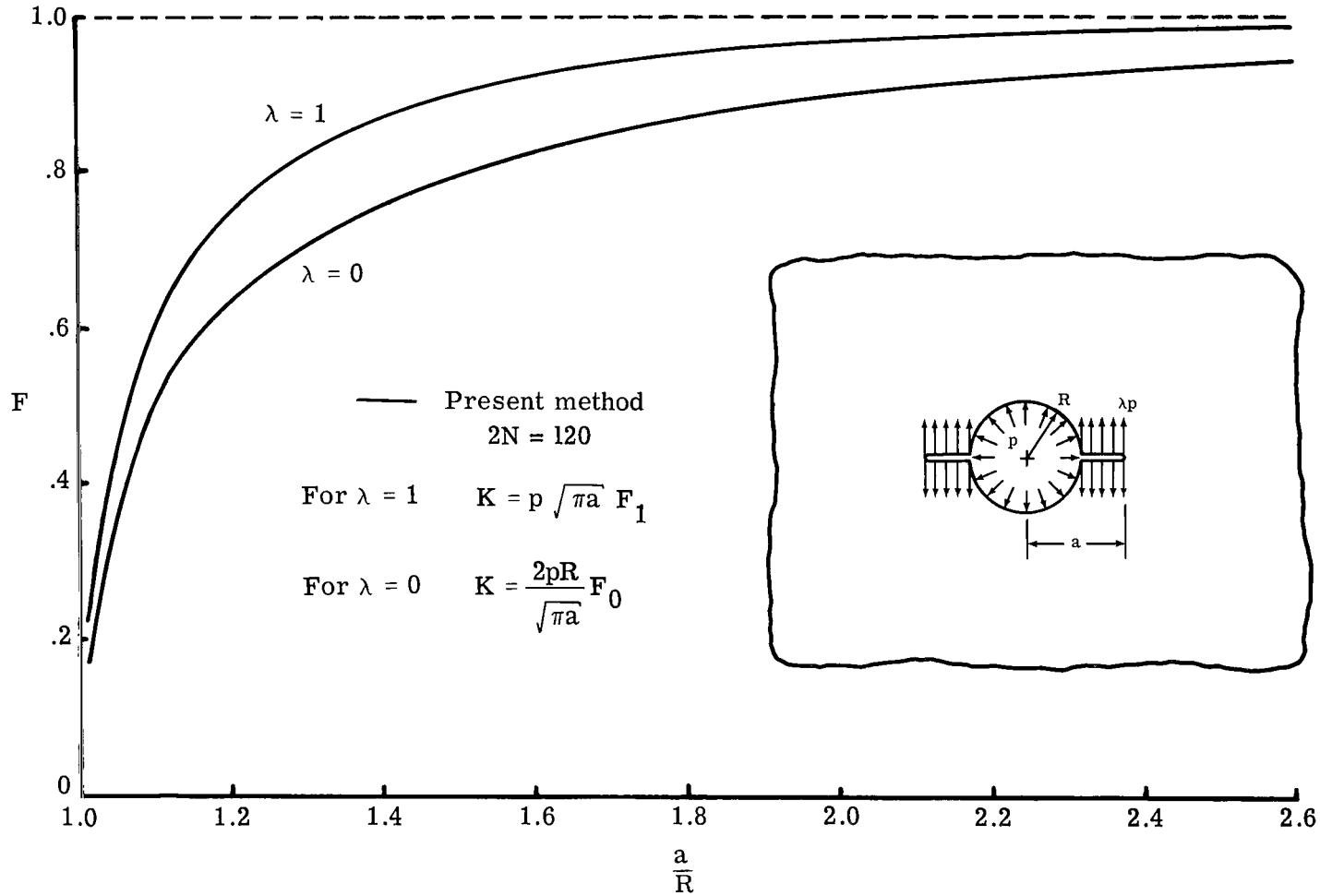

Figure 4.- Stress-intensity correction factors for cracks emanating from a circular hole in an infinite plate subjected to internal pressure.

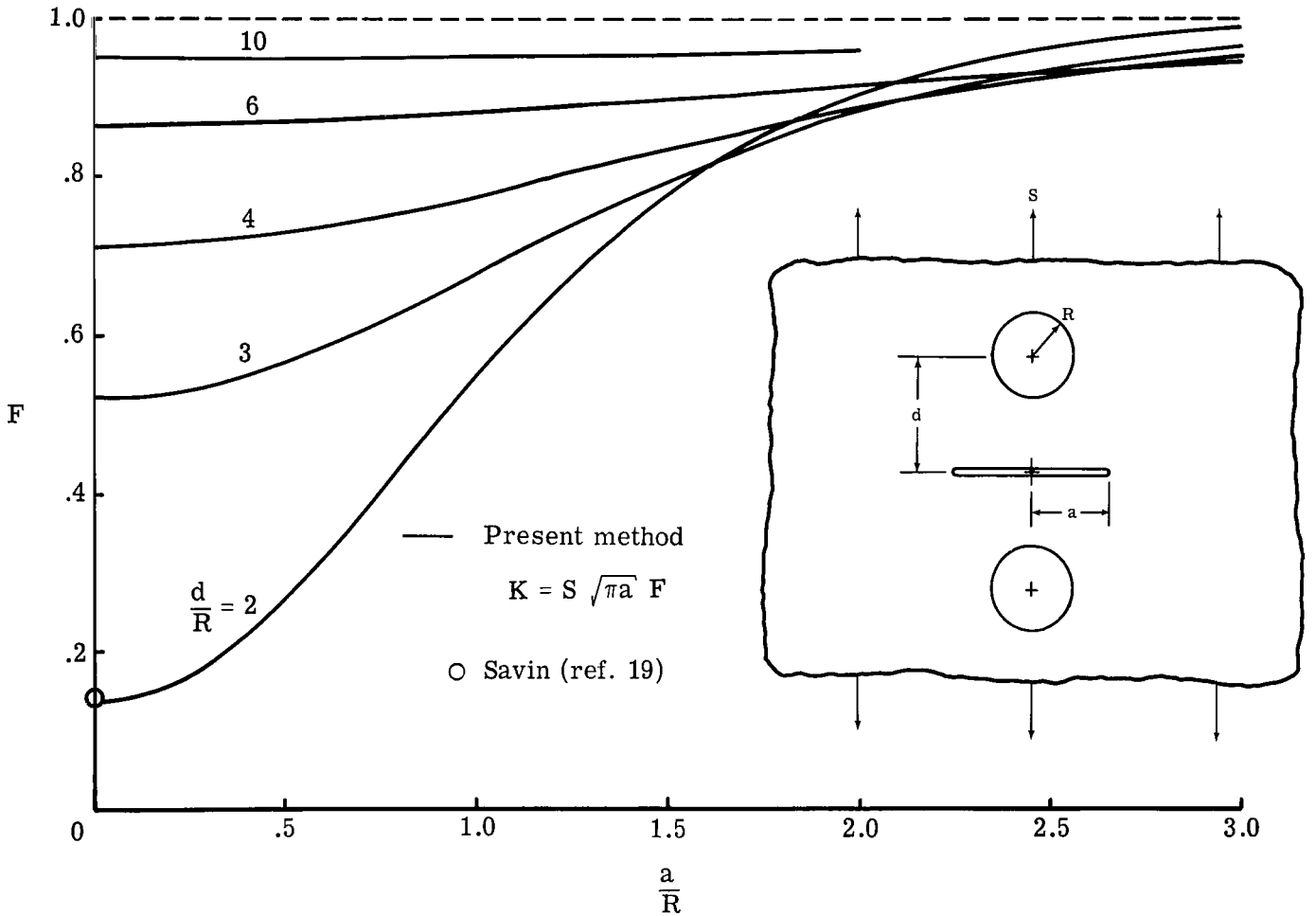

Figure 5.- Stress-intensity correction factors for a crack located between two circular holes in an infinite plate subjected to uniaxial stress.

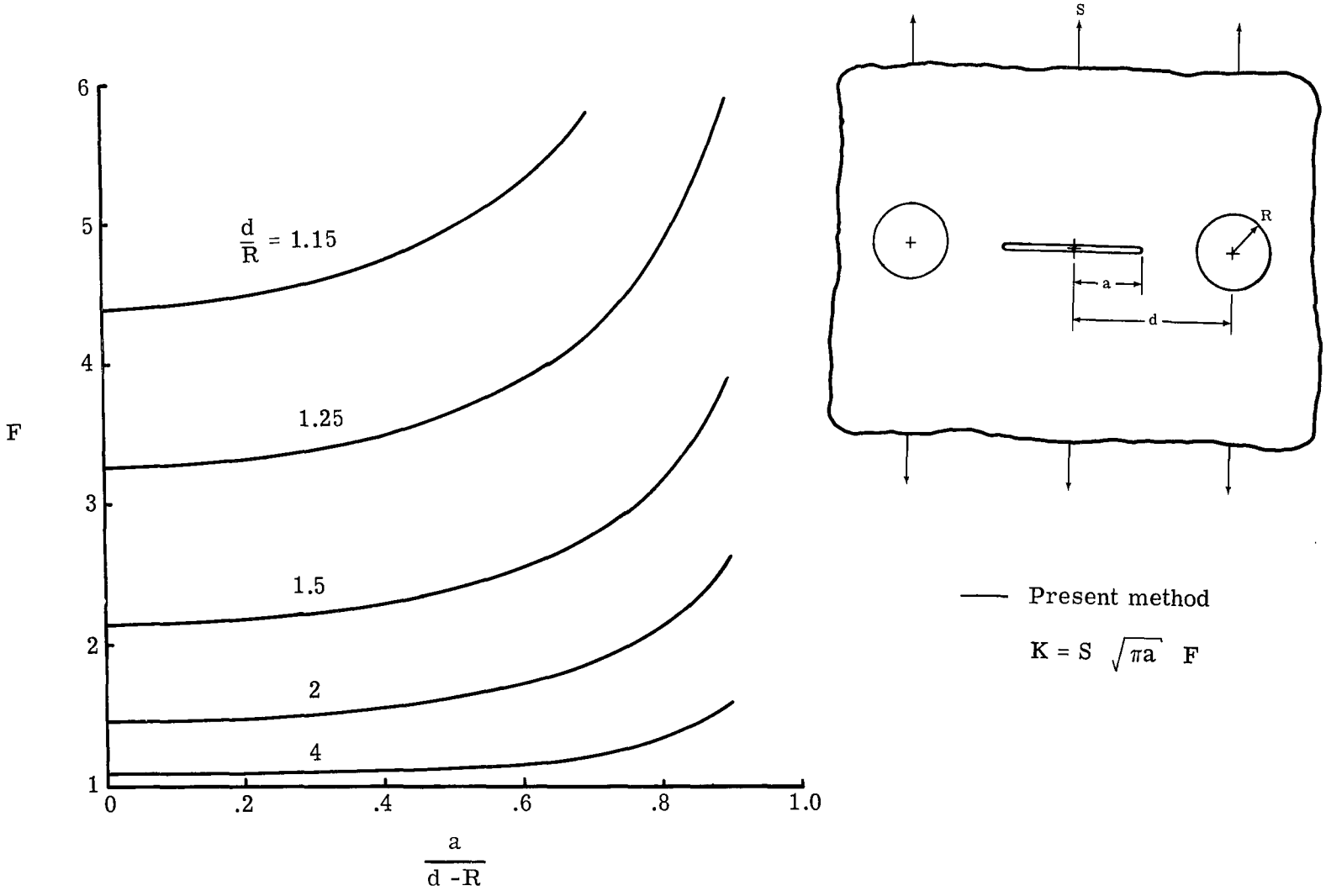

Figure 6.- Stress-intensity correction factors for a crack approaching two circular holes in an infinite plate subjected to uniaxial stress.

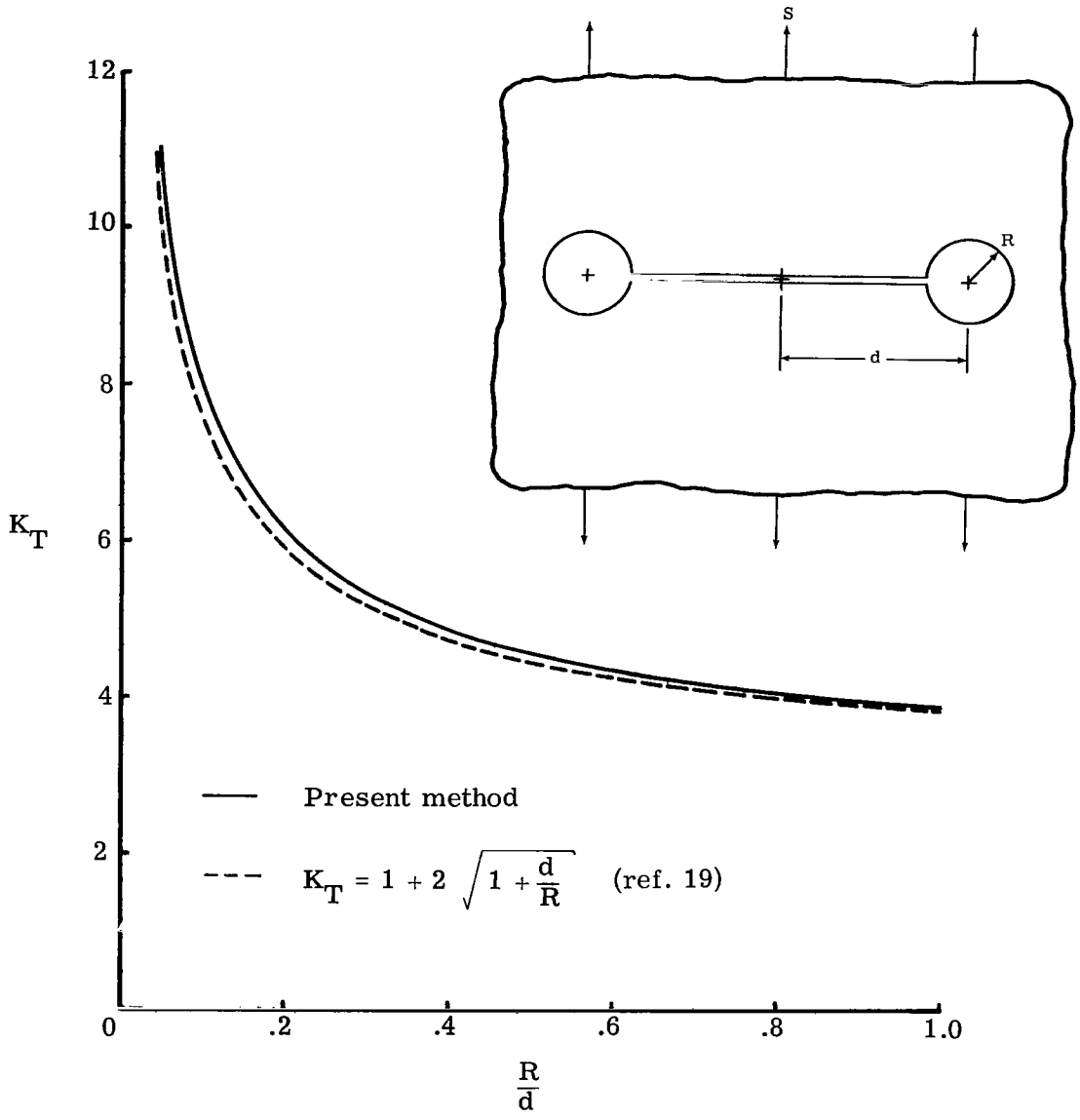

Figure 7.- Stress-concentration factor for two circular holes connected by a crack in an infinite plate subjected to uniaxial stress.

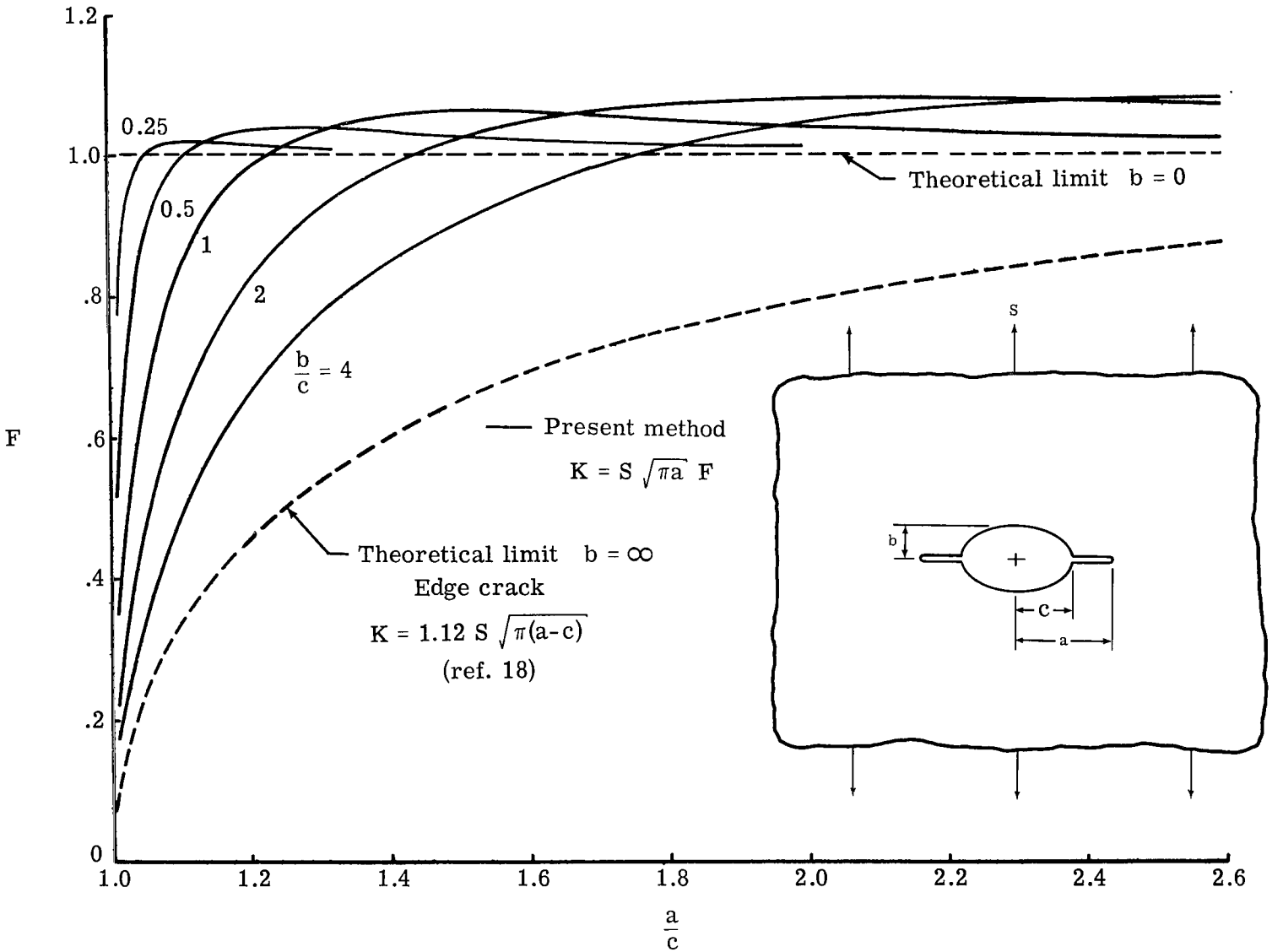

Figure 8.- Stress-intensity correction factors for cracks emanating from an elliptical hole in an infinite plate subjected to uniaxial stress.

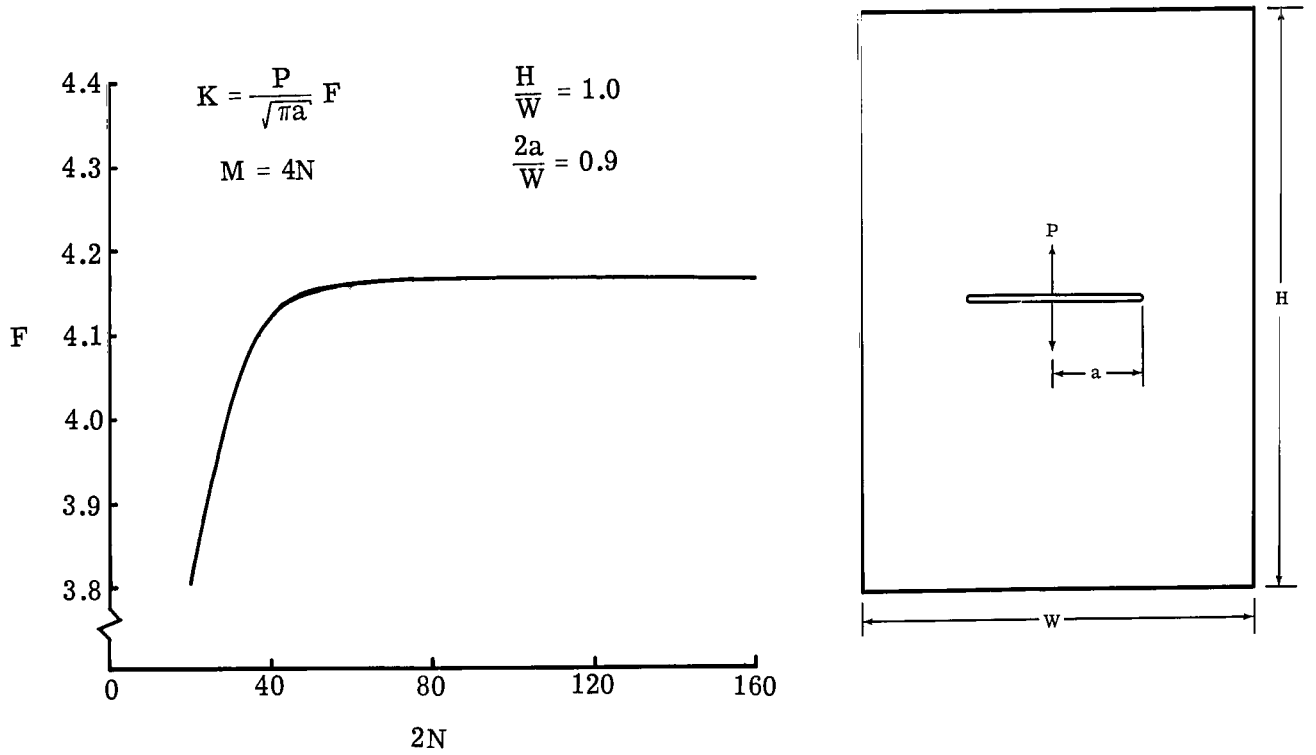

Figure 9.- Convergence curve for the problem of a wedge-force loaded crack in a rectangular plate.

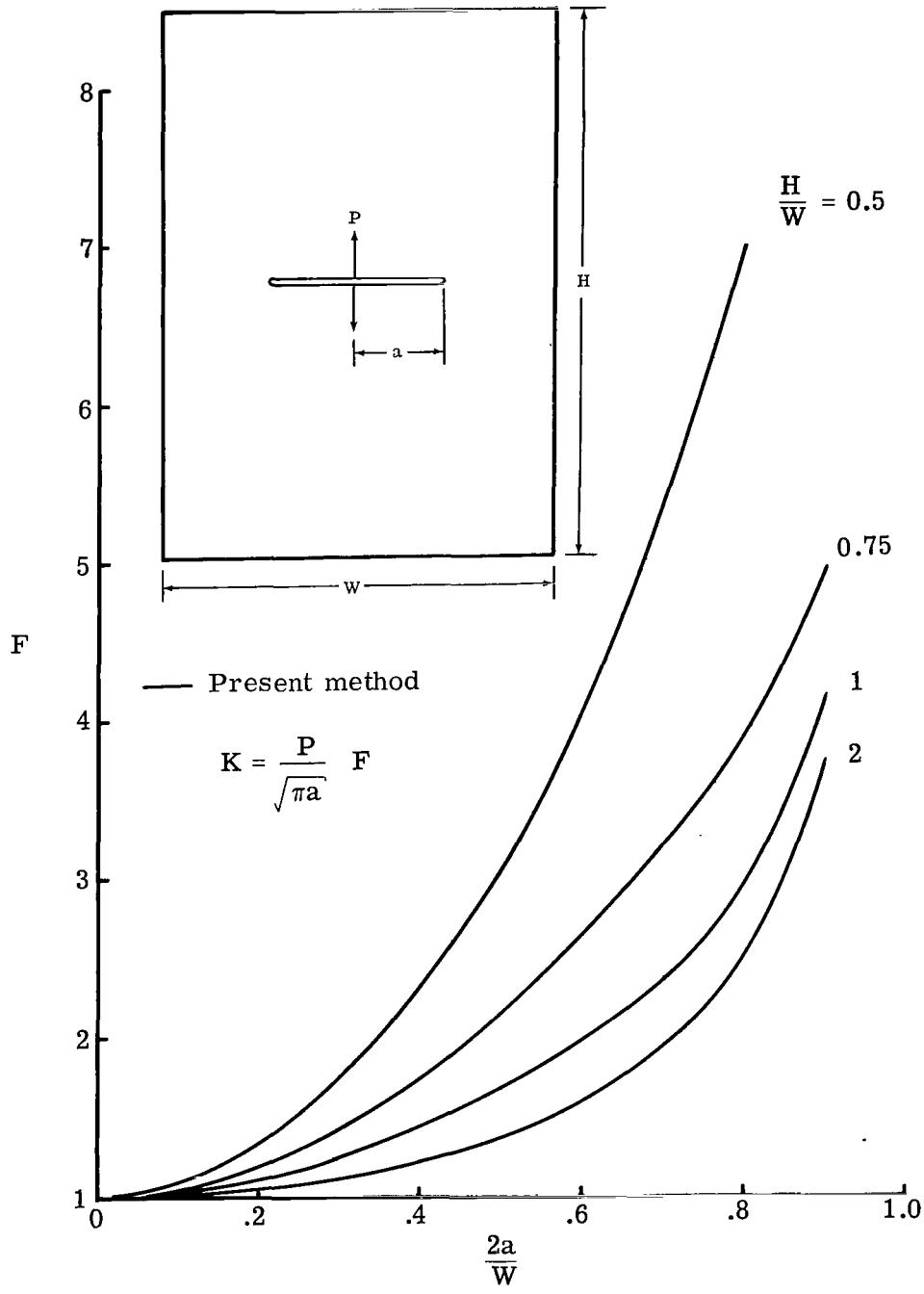

Figure 10.- Stress-intensity correction factors for a wedge-force loaded crack in a rectangular plate

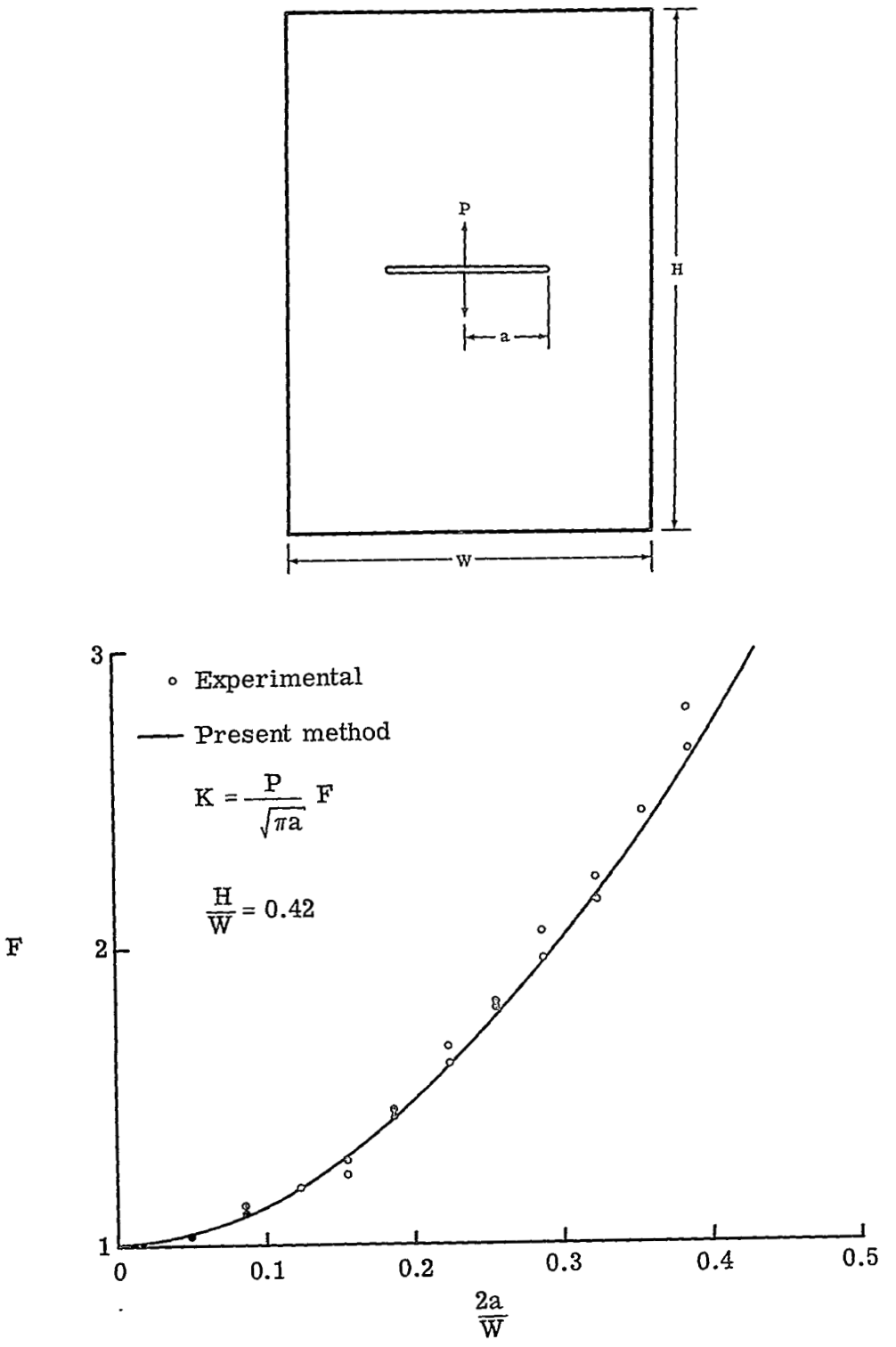

Figure 11.- Experimental and theoretical stress-intensity correction factors for a wedge-force loaded crack in a rectangular plate.

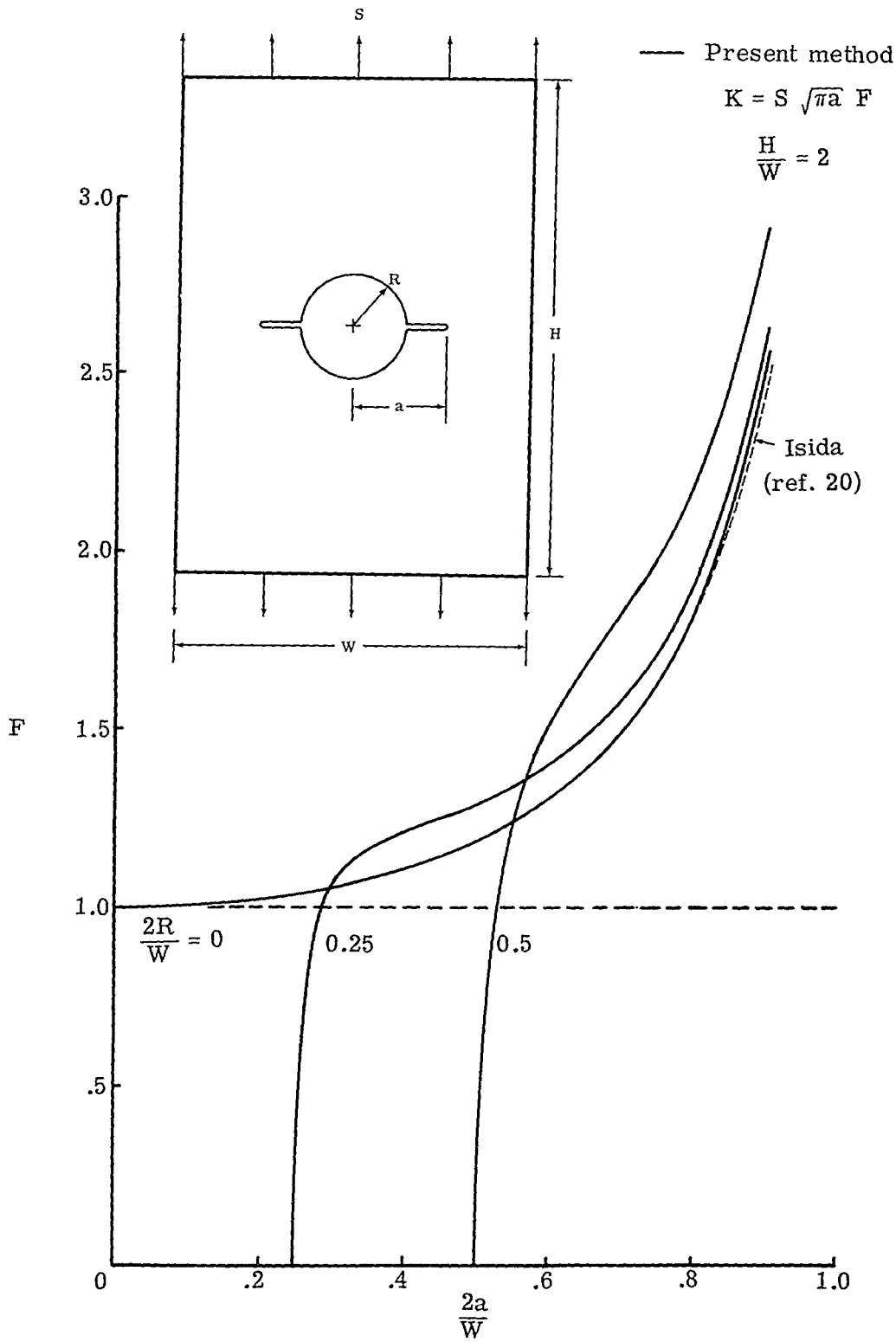

Figure 12.- Stress-intensity correction factors for cracks emanating from a circular hole in a rectangular plate subjected to uniaxial stress.

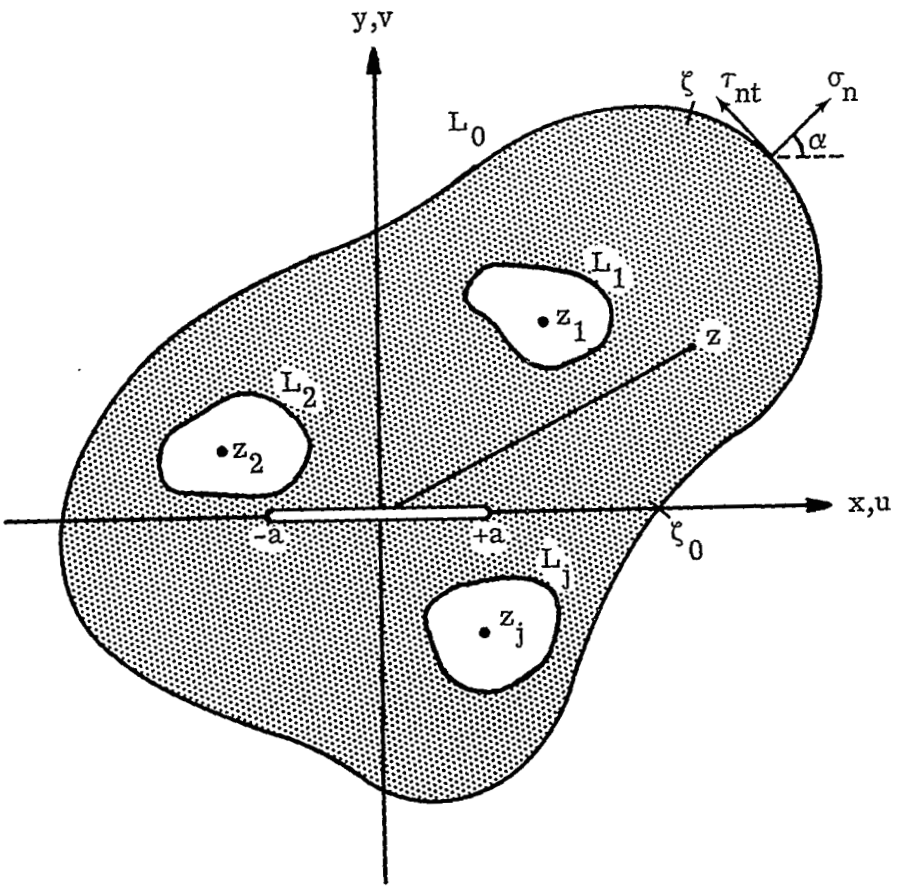

Figure 13.- Two-dimensional multiply-connected body containing a crack and subjected to surface tractions on the boundaries.

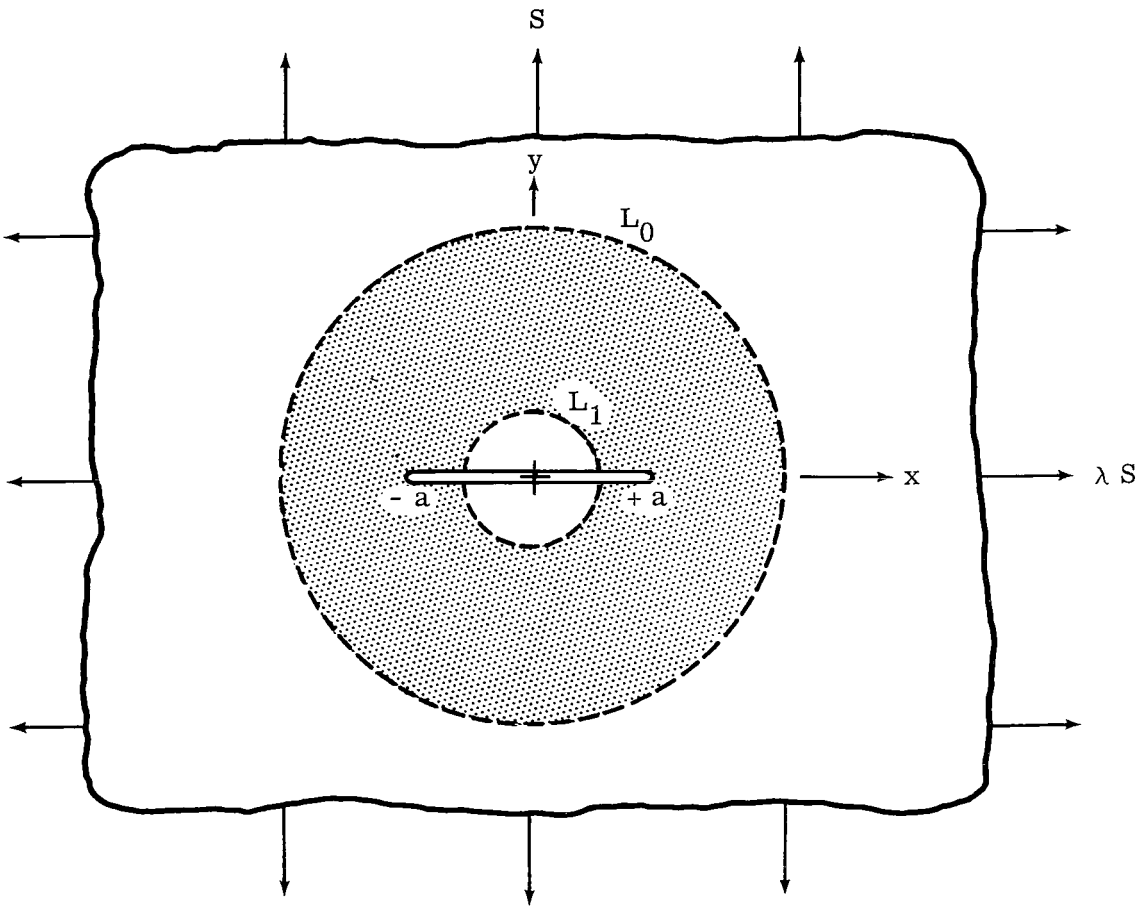

Figure 14.- Crack in an infinite plate subjected to biaxial stress.

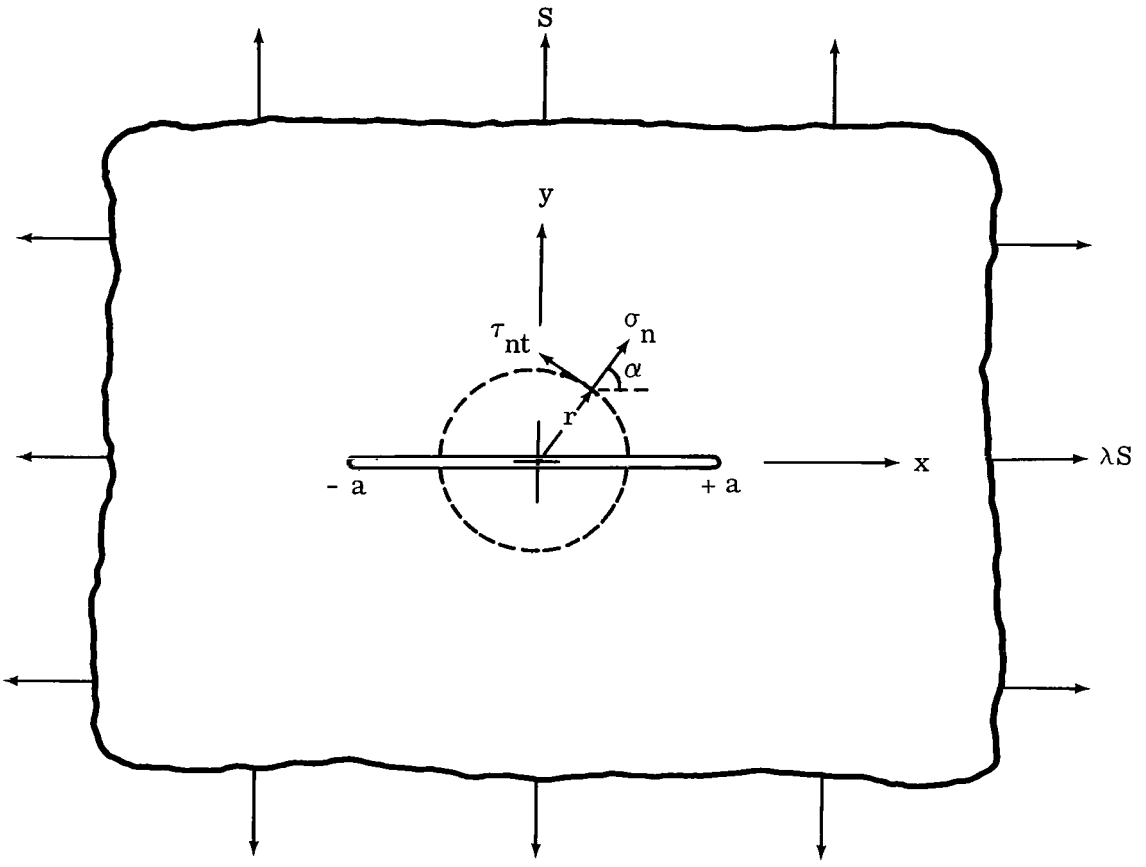

Figure 15.- Coordinate system used for the case of cracks emanating from a circular hole.